AD-A051 101 LITTLE (ARTHUR D) INC CAMBRIDGE MASS F/G 13/1
PRELIMINARY DESIGN OF A 10 KWE SOLAR HEATED OPEN BRAYTON-CYCLE --ETC(U)
NOV 77 N68305-76-C-0014
UNCLASSIFIED ADL-C-79516-F CEL-CR-78.003 NL

| OF |
AD
A051101

END
DATE FILMED
4 -78
DDC

12

CR 78.003

CIVIL ENGINEERING LABORATORY
Naval Construction Battalion Center
Port Hueneme, California

Sponsored by
NAVAL FACILITIES ENGINEERING COMMAND

PHASE I REPORT
PRELIMINARY DESIGN OF A 10 kWe SOLAR HEATED OPEN BRAYTON-CYCLE ENGINE

November 1977

An Investigation Conducted by

ARTHUR D. LITTLE, INC.
Cambridge, Massachusetts

N68305-76-C-0014

Approved for public release; distribution unlimited.

UNCLASSIFIED

SECURITY CLASSIFICATION OF THIS PAGE (When Data Entered)

(9) Final rept.

REPORT DOCUMENTATION PAGE

READ INSTRUCTIONS BEFORE COMPLETING FORM

(19) (18) CEL

1. REPORT NUMBER: CR-78.003
2. GOVT ACCESSION NO.
3. RECIPIENT'S CATALOG NUMBER

(6) 4. TITLE (and Subtitle): PHASE I REPORT, PRELIMINARY DESIGN OF A 10 kWe SOLAR HEATED OPEN BRAYTON-CYCLE ENGINE. Phase I.

5. TYPE OF REPORT & PERIOD COVERED: [redacted] (14)

6. PERFORMING ORG. REPORT NUMBER: 6-79516 ADL-C-79516-F

7. AUTHOR(s)

8. CONTRACT OR GRANT NUMBER(s): (15) N68305-76-C-0014

9. PERFORMING ORGANIZATION NAME AND ADDRESS
Arthur D. Little, Inc.
Acorn Park
Cambridge, MA 02140

10. PROGRAM ELEMENT, PROJECT, TASK AREA & WORK UNIT NUMBERS
62765N;F57.571; YF57.571.999; YF57.571.99.01.009C

11. CONTROLLING OFFICE NAME AND ADDRESS
Civil Engineering Laboratory
Naval Construction Battalion Center
Port Hueneme, CA 93043

(11) 12. REPORT DATE: Nov [redacted] 77

13. NUMBER OF PAGES: ~~75~~ (13) 76 pp

14. MONITORING AGENCY NAME & ADDRESS (if different from Controlling Office)
Naval Facilities Engineering Command
200 Stovall Street
Alexandria, VA 22332 (17)

15. SECURITY CLASS. (of this report): Unclassified

15a. DECLASSIFICATION/DOWNGRADING SCHEDULE

(16) 16. DISTRIBUTION STATEMENT (of this Report): F57571 YF57571999

17. DISTRIBUTION STATEMENT (of the abstract entered in Block 20, if different from Report)

DDC PROCESSED MAR 9 1978 F

18. SUPPLEMENTARY NOTES

19. KEY WORDS (Continue on reverse side if necessary and identify by block number)

Solar-electric; solar-thermal; Brayton-Cycle Engine; parabolic dish reflector

20. ABSTRACT (Continue on reverse side if necessary and identify by block number)

This report discusses the results of the first phase of a two-phase program to assess the applicability of electric power generation from solar energy at Naval bases, particularly advanced bases which require small, mobile systems not under development in the civilian sector.

For purposes of establishing a baseline system against which

DD FORM 1 JAN 73 1473 EDITION OF 1 NOV 65 IS OBSOLETE

UNCLASSIFIED

SECURITY CLASSIFICATION OF THIS PAGE (When Data Entered)

208 850

UNCLASSIFIED

Block 20 cont'd

the costs and benefits of various solar-to-electric energy conversion processes can be compared, an open-cycle air turbine/generator set was chosen with tracking parabolic dish reflector to focus direct solar radiation onto a collector/heat exchanger providing heat for the engine. Preliminary system designs and cost estimates were prepared for the solar "fired" open-cycle air turbine generator meeting the following design goals:

Power Output:	10 KWe, 60Hz, 120V
Weight:	Less than 10,000 lb
Structure:	Capable of being dismantled and packaged in 8'x8'x20' containers
General:	(a) Withstand a "reasonable" amount of abuse during erection by Seabees.
	(b) No energy storage; system tied to grid.

Preliminary design parameters determined for the system were:

Midday Power Output:	10 KWe, 120V, 60Hz
Operating Temperature:	1300°F
Concentration Ratio:	400/1
Dish Diameter:	30 ft.
Overall Efficiency:	17.6%

Where possible, technical and cost information for the various subsystems was obtained by direct contacts with firms in related product areas, in particular, firms in the antenna field and firms producing small Brayton-cycle engines. A cost of $42,000 per unit estimate was projected for a production level of 1,000 units per year. At production levels high enough to warrant true assembly line techniques, optimistic cost estimates were as low as $12,000 per unit. Based upon the capital cost estimate of $42,000 per unit and upon overall annual performance of the unit at a site with favorable insolation, it was projected that cost of power from the system would be $0.27/Kwh (270 mils/Kwh).

UNCLASSIFIED

TABLE OF CONTENTS

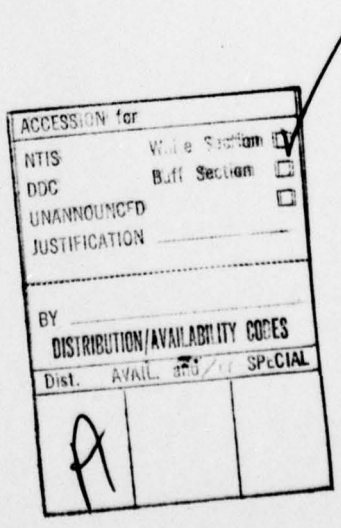

TABLE OF CONTENTS (Continued)

LIST OF FIGURES

LIST OF TABLES

1. INTRODUCTION AND SUMMARY

This report discusses the results of the first phase of a two-phase program to assess the applicability of electric power generation from solar energy at Naval bases, particularly advanced bases which require small, mobile systems not under development in the civilian sector. The two program phases are:

Phase 1: Preliminary Definition of the Cost/Performance Characteristics of a Solar-Powered Open Brayton-Cycle Engine

Phase 2: Comparison of Solar Power System Options

Numerous approaches are available for converting solar energy to electric power, such as photovoltaics, Rankine-cycle engines with flat plate collectors, and steam engines with parabolic trough collectors. For purposes of establishing a baseline system against which the costs and benefits of these various approaches can be compared, CEL chose an open-cycle air turbine/generator set with a tracking parabolic dish reflector to focus direct solar radiation onto a collector/heat exchanger providing heat for the engine.

The open Brayton-cycle engine has a number of potential advantages for these mobile power applications:

- It uses air as the "working fluid," which eliminates the need for a sealed system such as required by Rankine-cycle, Stirling, or closed Brayton-cycle engines.
- With an open cycle, no water- or air-cooled heat rejection heat exchanger is required (such as the condenser of a Rankine-cycle engine loop).
- Small Brayton-cycle engines (both open and closed) have been developed as part of DOD- and NASA-sponsored projects.
- Using high levels of concentration allows for generating high temperature levels and, thereby, achieving efficient engine operation.

The objective of the Phase 1 effort was to prepare preliminary system designs and cost estimates for a solar "fired" open-cycle air turbine generator with the following design goals:

Power Output:	10 kWe, 60 Hz, 120 V
Weight:	Less than 10,000 lb
Structure:	Capable of being dismantled and packaged in $8' \times 8' \times 20'$ containers
General:	Withstand a "reasonable" amount of abuse during erection by Seabees.

This system must be portable to the extent that it can be easily dismantled and erected by Seabees using their standard field equipment. This requirement, in turn, requires rugged components and a system design which is not too sensitive to a reasonable amount of accidental abuse. For purposes of this preliminary design study, energy storage was not considered and the system was assumed to be supplementing a conventional power system (such as a diesel generator power plant) on a demand basis. Off-design performance characteristics of the solar-powered

system were estimated and used to predict daily variations in power output using clear-day insolation plots provided by CEL. The determination of seasonal performance characteristics based on measured direct insolation values was not, however, within the scope of this first-phase program.

Selection of the solar-powered open Brayton-cycle engine as a baseline system serves several purposes. First, a preliminary design of this system results in a fairly detailed knowledge of the state-of-the-art of solar technologies involved in solar thermal power generation (reflector materials, tracking systems, receiver design considerations, etc.). Second, reasonable cost and performance estimates are obtained for one of the more promising system options for a mobile solar power source. Third, the knowledge gained and information gathered would result in a much improved ability to compare the "baseline" system with other system options, conventional and solar powered, for electric power generation at advanced bases (which will be considered in Phase 2).

The solar "fired" Brayton-cycle engine consists of three major subsystems:

- A *tracking reflector* (parabolic or linear), which concentrates the direct portion of the solar energy on a receiver.
- A *receiver*, which absorbs concentrated solar energy at elevated temperatures and transfers this energy to the air stream of the Brayton-cycle engine. (The receiver essentially takes the place of the combustion chamber of a fuel-fired Brayton-cycle engine.)
- An open Brayton-cycle engine (turbine/compressor), which uses ambient air as the working fluid. For high engine efficiency levels, a regenerative cycle will have to be used.

Conventional Brayton-cycle engines usually operate at a peak air temperature of about 1600°F. Thermal efficiency would improve at higher temperature levels, but material problems become increasingly difficult.

In principle, a solar-heated Brayton-cycle engine could also operate at 1600°F; in fact, several studies have been made on such systems. In practice, however, achieving such high temperatures with a solar-heated system requires the use of very high levels of concentration (probably 1500:1 to 2000:1), and the necessary precision in the reflector contours and tracking accuracy are unlikely to be consistent with the overall program goals of a rugged, mobile unit capable of erection and maintenance by normal Navy personnel.

For the purposes of this program, the performance characteristics of the critical subsystems were estimated as a function of important parameters such as operating temperature levels, concentration ratio, and receiver thermal characteristics. The subsystem performance characteristics were used to calculate overall system performance levels for a range of system design options. With a concentrating system of reasonable precision, the optimum temperature of operation appears to be in the 1200-1400°F range. The preliminary system design is based on the use of a tracking parabolic concentrator with a polar mount that focuses solar energy on a single receiver at the focal point. Hot air generated in the receiver flows through a duct to the engine/generator, which is mounted on the rear of the parabolic dish. This mounting arrangement eliminates the need for flexible joints in the air distribution system. Preliminary design parameters for this system are as follows:

Midday Power Output — 10 kWe, 120V, 60 Hz
Operating Temperature — 1300°F
Concentration Ratio — 400:1
Dish Diameter — 30 ft
Dish Area — 705 ft^2
Overall Efficiency — 17.6%
Receiver Aperture Diameter — 1.5 ft

While the concentration ratio of 400:1 is lower than that assumed by some other studies, higher ratios require increasing levels of precision in the reflector and tracking systems and result in only modest improvements in system performance. This concentration level was chosen to permit a reasonable compromise between efficiency and reliability in a field system.

Where possible, technical and cost information for the various subsystems was obtained by direct contacts with firms in related product areas. In particular, firms in the microwave antenna field were contacted for inputs on the reflector system, and firms making small fuel- and isotope-powered Brayton-cycle engines provided cost/performance information on the engine options.

These inputs were combined with Arthur D. Little projections to estimate the cost of the solar-powered unit if it were produced in quantities of 1000 per year.

The resultant system cost estimate was $42,000 per unit once the R&D effort required to produce an appropriate recuperated open Brayton-cycle engine is completed. Since the technology and design for the reflector and receiver are straightforward, these subsystems would probably not require a substantial R&D effort. The cost might be reduced by a factor of 4-6 if one or more of the subsystems were being manufactured in large quantities for some other application; 1000 units is considered a small quantity by most manufacturers.

A detailed economic evaluation of a solar-powered unit requires the calculation of annual power output (kWh) based on measured insolation and allowing for poor days as well as clear days. Preliminary seasonal performance estimates combined with the above cost projection indicate that the cost of power from this system would be $0.27/kWh in areas of favorable insolation (assuming 10% capital costs). This cost of power is still substantially higher than that from conventional generating equipment. As previously noted, the cost of this system could be significantly reduced if it were in larger scale production than the assumed 1000 units per year. It appears, therefore, that the economic viability of this approach to solar power generation is contingent upon such increases in production levels.

2. SYSTEM OPTIONS CONSIDERED

Initial analysis of open Brayton-cycle engines indicated that peak cycle temperatures of over 1000°F (preferably over 1200°F) would be necessary for the engine to have an efficiency of at least 10%. These elevated temperature levels can be generated from solar energy using a combination of solar concentration and optical approaches to reducing receiver heat losses.

2.1 Concentrator Options

Either of the following basic concentrator types can be used to focus solar energy:

- *Point concentrators* track the sun in two planes and focus the solar energy on a focal plane in a circular pattern. The energy being focused is collected over a circular aperture area which increases as the square of the radius. Concentrators of this type include parabolic dishes and circular Fresnel lenses. Point concentrators can achieve concentration levels as high as 1000-2000:1.
- *Linear concentrators* usually track the sun in one plane only and focus the solar radiation on a line whose width is a function of the concentration ratio. Concentrators of this type include parabolic troughs, linear slat configurations, and linear Fresnel lenses. Linear concentrators can achieve concentration levels of between 20:1 and 40:1.*

With proper receiver design, both types of concentrators can achieve the required temperature levels. Linear concentrators have the advantage of having to track in only one plane and are therefore simpler than point concentrators from a structural, mechanical, and control standpoint. Point concentrators, on the other hand, can achieve higher concentration ratios and, hence, higher temperatures. Because they continuously follow the sun, they incur no cosine-loss effects as with most linear systems.

Since both concentrator options appear to offer advantages, both were considered during the initial stages of the project so that the final selection of concentrator/receiver configuration would be the most appropriate for the proposed application.

2.2 Receiver Options

The thermal performance of a solar concentrating system is critically dependent on the thermal characteristics of the receiver onto which the solar flux is directed. Figure 2.1 shows three of the options available for configuring the receiver of the power system.

(a) *Black Body Receiver* — The black body receiver consists of a cavity into which the reflected radiation is concentrated. Assuming this cavity is well insulated, the primary energy loss is by reradiation back through the cavity opening.

(b) *One Radiation Shield* — The radiation heat loss from the black body receiver can be reduced approximately 50% if a cover is placed over the cavity opening which transmits

* These ratios are practical limits set by the requirements for contour and tracking accuracy. Theoretical limits are significantly higher, as indicated in Reference 1.

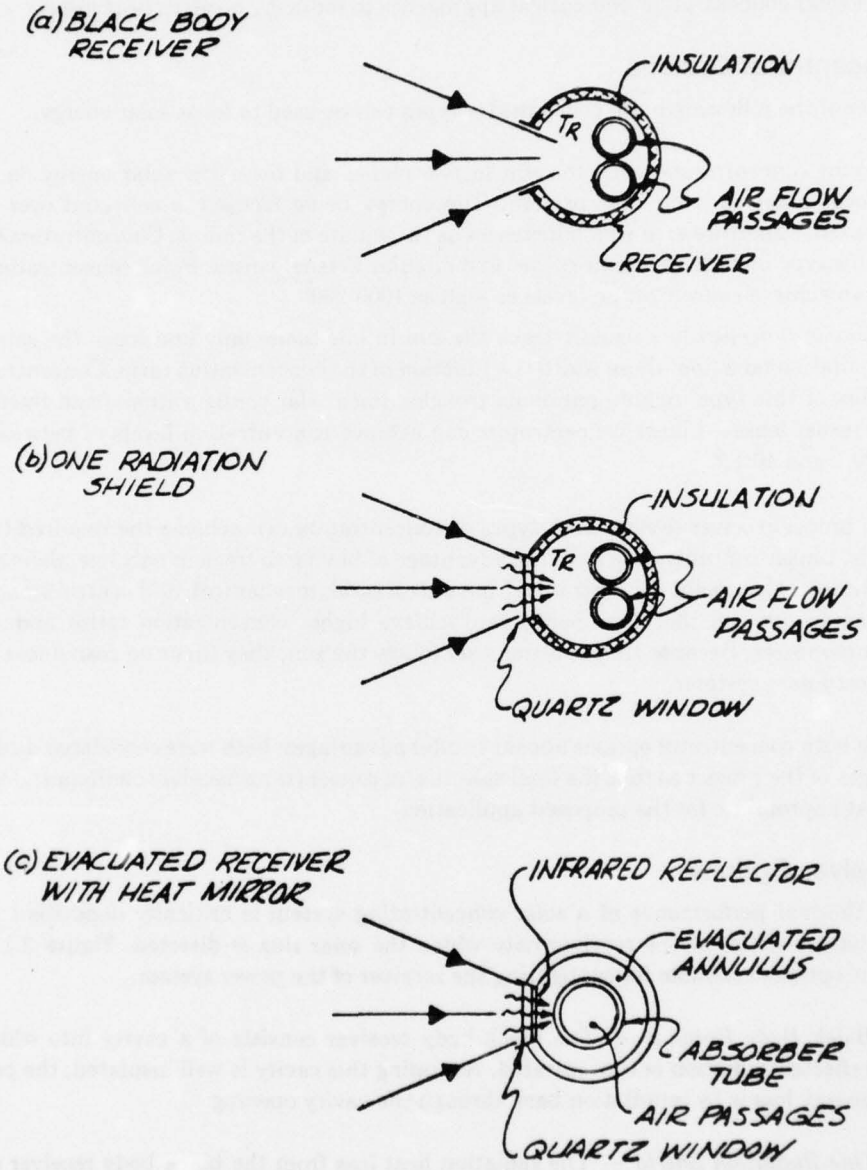

FIGURE 2.1 RECEIVER DESIGN OPTIONS

a high percentage of the short-wavelength solar radiation and is opaque to infrared radiation from inside the cavity. Both glass and quartz have these optical characteristics and could function as a radiation shield. The primary disadvantage of this approach is that 6-12% of the incident energy will be reflected or absorbed by the window.

(c) *Heat Mirror* — Reradiation heat losses could be further reduced by coating the inner surface of the window with an infrared reflector which transmits most of the solar radiation but reflects infrared radiation. Such coatings include tin oxide, indium oxide, and titanium oxide multi-layers.(2,3,4) The disadvantages of this approach include transmission losses of about 15% and the fact that the use of heat mirrors in this application is untried. Evacuation of the space between the absorber and the reflecting window is desirable if possible.

2.3 Concentrator/Receiver Efficiency

The heat loss mechanisms which reduce the efficiency with which focused solar flux is collected by the receiver include:

- Reradiation losses back through the receiver aperture;
- Conduction losses through the insulation on the sides and back of the receiver; and
- Convection losses over the receiver aperture area.

At the temperature levels of prime consideration (in excess of 1000°F), reradiation predominates over other heat loss mechanisms. For example, at 1200°F the black body radiation heat transfer is over 13,000 Btu/hr-ft², while convection heat transfer losses would be on the order of 2000 Btu/hr-ft². For purposes of screening the various concentrator/receiver design options, only the radiation heat loss mechanism was considered. The final system design must, however, take into consideration all heat loss mechanisms.

The screening analysis was undertaken to answer several important questions:

- Is it possible to reduce the required level of solar concentration to that achievable with linear systems by using a heat mirror to greatly reduce reradiation losses?
- If a point concentrator is used, under what conditions does the use of a transparent radiation shield (quartz cover) improve receiver thermal efficiency?
- What levels of concentration are required to efficiently achieve the operating temperatures required by the engine/generator?

It is necessary to address these questions in order to identify the most appropriate system configuration for the more detailed system analysis and preliminary design effort.

The efficiency of the concentrator/receiver subsystem is defined as:

$$\eta = \frac{\text{Heat Absorbed in Receiver}}{\text{Direct Solar Flux Incident on Concentrator}}$$

$$\eta = \eta_o - \frac{1}{(N+1)(C)} \times \frac{\epsilon\, q_{bb}(T_R)}{q_D}$$

where:

η_O = Optical efficiency, i.e., the percentage of the incident radiation which is absorbed in the receiver cavity after taking into account concentrator surface reflectivity, optical losses due to surface contour or tracking errors, and transmission losses into the receiver cavity.

N = Number of transparent radiation shields over the receiver aperture.

$q_{bb}(T_R)$ = Black body reradiation loss from the receiver in Btu/hr-ft².

ϵ = Effective emissivity of the receiver.

q_D = Direct solar flux incident on the concentrator aperture in Btu/hr-ft².

C = Geometric concentration ratio, defined as the concentrator aperture area over the receiver aperture area.

Collector system efficiency was calculated for concentration ratios in two ranges:

- C = 30:1 — This concentration ratio is achievable with an accurate linear focusing system.
- C = 200:1, 400:1, 800:1 — Parabolic dish concentrators with relatively loose tolerances (as discussed in Section 2.4) can achieve these concentration ratios. Higher levels of concentration could be obtained with more precise equipment but should not be necessary.

Efficiency calculations were based on the following assumptions:

(a) *Solar Flux* — All calculations were based on an assumed clear-day insolation value of 275 Btu/hr-ft².

(b) *Concentrator* — Reflectivity = 0.85; optical errors = 5%.

(c) *Receiver*

Case 1: Black body receiver

Transmission: $\tau = 1.0$
Absorptivity: $\alpha = 0.98$
Radiation shields: N = 0
Optical efficiency: $\eta_O = 0.785$

Case 2: Black body receiver with quartz shield

Transmission: $\tau = 0.94$
Absorptivity: $\alpha = 0.98$
Radiation shield: N = 1
Optical efficiency: $\eta_O = 0.736$

Case 3: Receiver with heat mirror

Transmission: $\tau = 0.85$

Absorptivity: $\alpha = 0.98$

Radiation Shield: $\rho = 0.80$ (equivalent to 4 radiation shields)

Optical efficiency: $\eta_O = 0.666$

The "heat mirror" in Case 3 reflects 80% of the infrared reradiation from the receiver cavity, which is equivalent to having four heat shields. More effective heat mirrors have been tested, several of which reflect 90% of the energy in the infrared spectrum[2,3] associated with lower heat-source temperatures (70-400°F). As the temperature of the heat source increases, there is less and less difference in the wavelength spectra between the solar flux and the re-emitted energy. This makes it increasingly difficult to produce heat mirrors with such a sharp spectral cutoff that they are both good transmitters of solar radiation and good reflectors of the re-emitted infrared energy. A ρ_{IR} of 80% appears to be consistent with near-term technology, given the relatively high temperatures of the heat source.

Figure 2.2 shows results for several representative concentrator systems. It is clear that linear systems using a concentration ratio of 30:1 would require very effective heat mirrors to efficiently achieve temperature levels in excess of 1000°F required for the open Brayton-cycle engine.

For point concentrator systems, the required temperatures can be achieved at relatively modest concentration levels, particularly if a quartz cover is used to reduce reradiation losses.

Figure 2.3 shows the effect of solar concentration on efficiency for a point concentrator. These curves apply to temperatures which engine analysis (Section 3.3) indicates as being in the range of primary interest. Note that efficiency increases rapidly with concentration ratio at low to modest levels of concentration (100-200). At ratios significantly above 400-500:1, the rate of increase in efficiency is quite small.

Figure 2.4 shows efficiency as a function of temperature for concentrating systems using receivers with and without a quartz window. At C = 200, the quartz window significantly improves efficiency throughout the temperature range of interest. At C = 400, however, the window is beneficial only above 1200°F, and then only marginally so. The indicated efficiencies are probably optimistic for the quartz window case at temperatures above 1200°F, since an increasing percentage of the reradiation falls in the near-infrared wavelengths transmitted by the window. This effect is shown in Figure 2.5 for the case of reradiation from a 1000°K (1340°F) cavity.

2.4 Effect of Optical Errors

The analysis leading to the concentrator/receiver efficiency curves of Figures 2.2-2.4 was based on assumed optical errors of 5%, meaning that 5% of the reflected energy was misdirected and never reached the receiver. In this case optical errors refer to:

- Errors in tracking the sun, so that some of the redirected energy does not impinge on the focal plane;
- Local surface contour errors in the reflector surface; and
- Errors in positioning the receiver at the focal point.

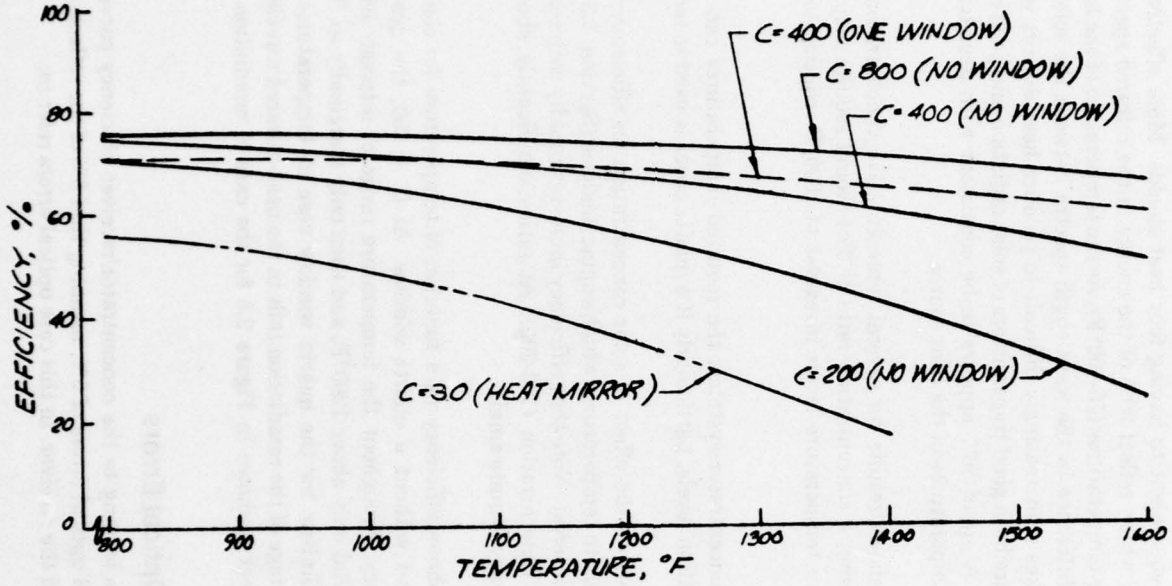

FIGURE 2.2 VARIATION OF CONCENTRATOR/RECEIVER SYSTEM EFFICIENCY WITH TEMPERATURE

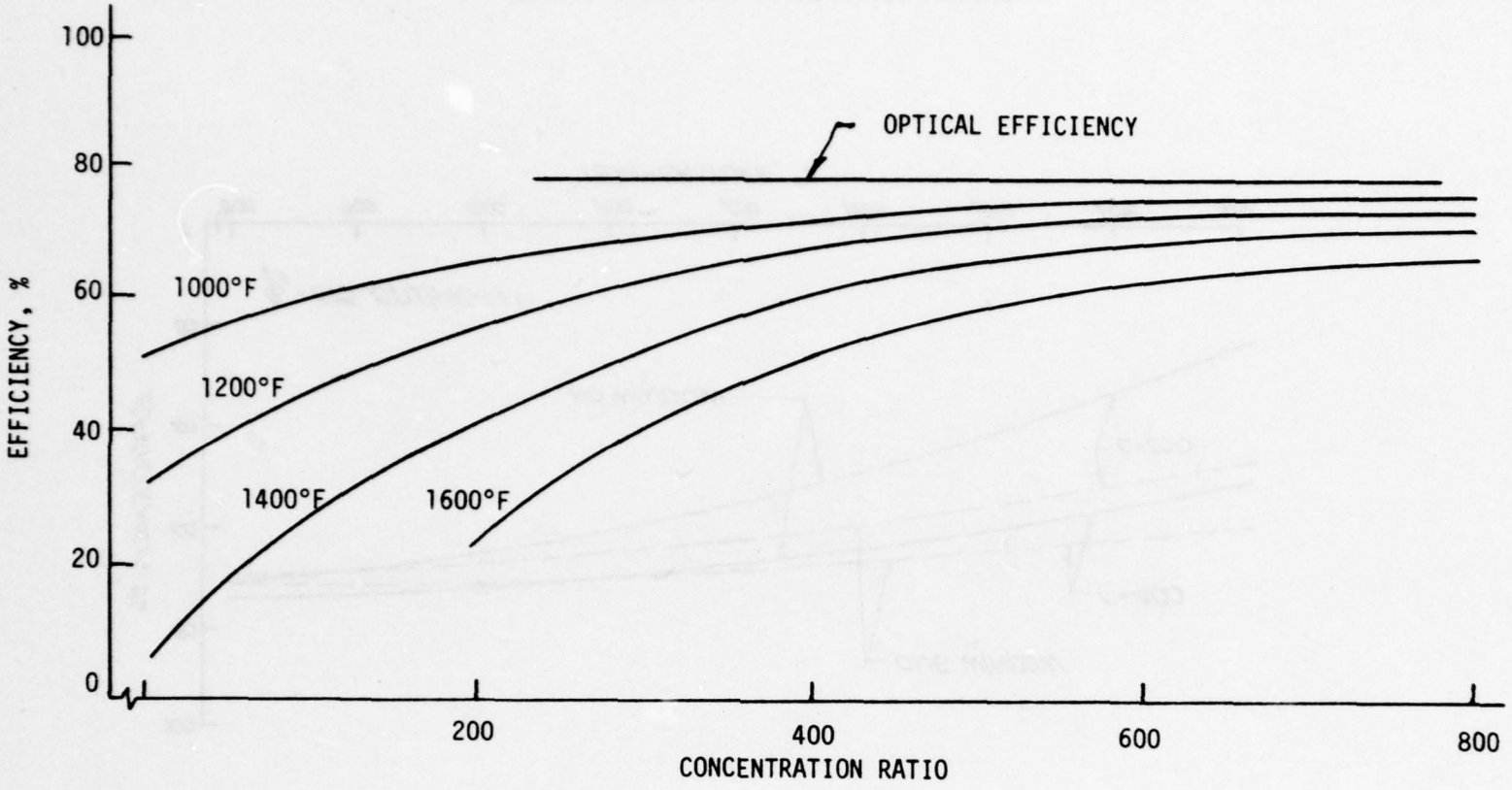

FIGURE 2.3 EFFECT OF CONCENTRATION RATIO ON CONCENTRATOR/RECEIVER SYSTEM EFFICIENCY

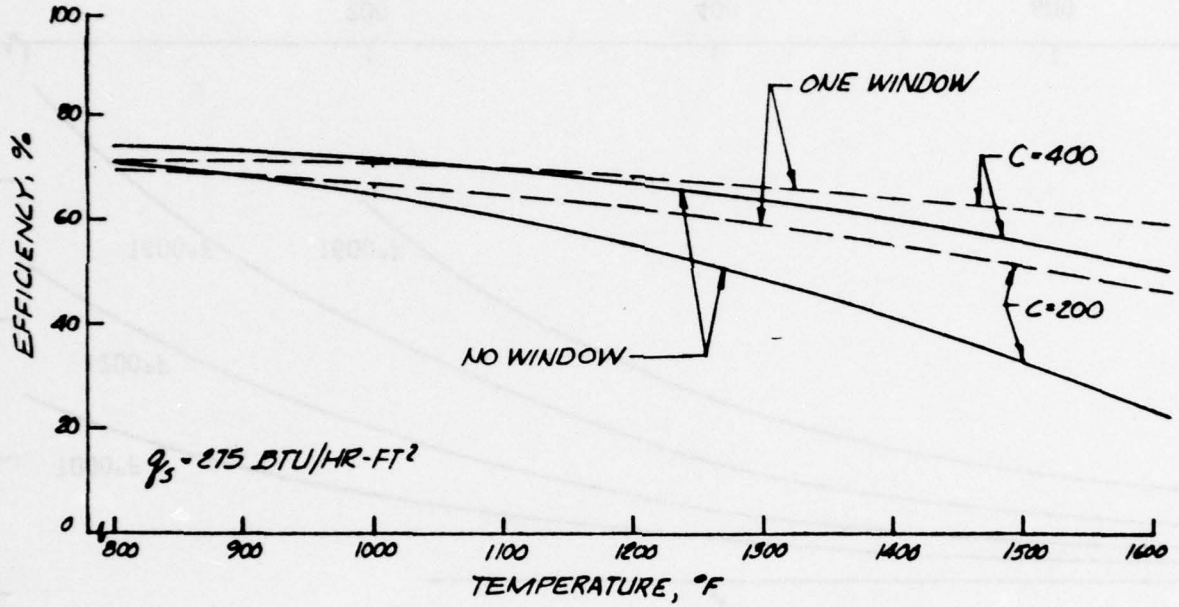

FIGURE 2.4 EFFECT OF RECEIVER "WINDOW" ON EFFICIENCY

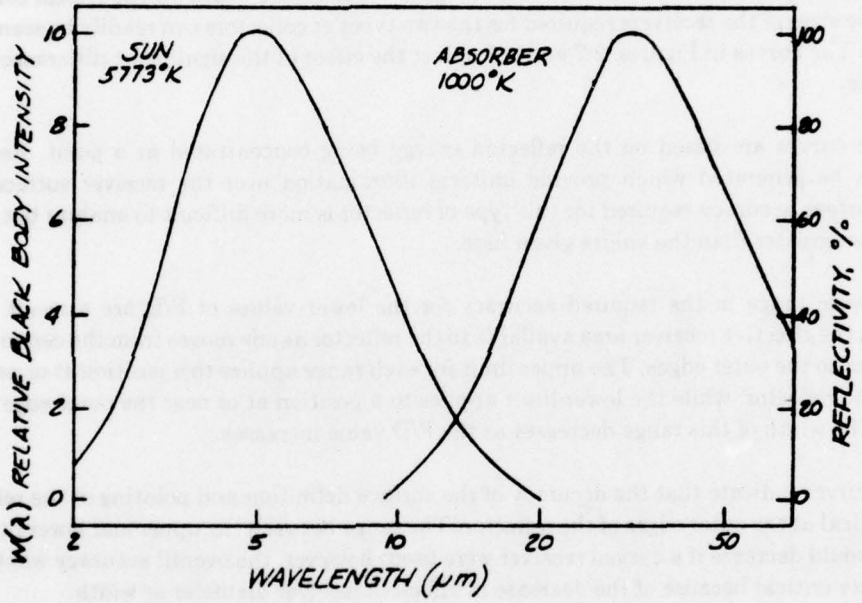

FIGURE 2.5 BLACK BODY WAVELENGTH SPECTRUM FOR AN ABSORBER OPERATING AT 1000°K (1340°F)

There will always be errors of this kind, and their importance will tend to increase with the concentration ratio. The precision of the optical system must keep pace with the concentration ratio to keep optical losses within any preset limit. Greater precision in geometry and tracking, in turn, increases costs and makes it more difficult to design a system that meets the overall requirements of a reliable, mobile solar power unit. The required accuracy of the pointing system and surface definition of the reflector can, therefore, significantly affect the type of concentrator and concentration ratio selected.

The relationship between accuracy and concentration ratio for a parabolic trough collector and a parabolic point collector is indicated in Figures 2.6 and 2.7, respectively. A schematic representation of the two types of collectors having a concentration ratio of 100 for different F/D ratios is also shown in Figure 2.8. The F/D ratio is defined as the focal length over aperture diameter for the point concentrator and focal length over aperture width for the trough collector. The relative sizes of the receivers required for the two types of collectors can readily be seen in the schematic. The curves in Figures 2.7 and 2.8 reflect the effect of the significant difference in the receiver size.

These curves are based on the reflected energy being concentrated at a point. Reflector shapes can be generated which provide uniform illumination over the receiver surface. The pointing/surface accuracy required for this type of reflector is more difficult to analyze but would be somewhat greater than the values given here.

The wide range in the required accuracy for the lower values of F/D are a result of the decrease in the effective receiver area available to the reflector as one moves from the center of the concentrator to the outer edges. The upper limit for each range applies to a position at or near the center of the reflector, while the lower limit applies to a position at or near the outer edge of the reflector. The width of this range decreases as the F/D value increases.

The curves indicate that the accuracy of the surface definition and pointing of the reflector is more critical at the outer edges of the reflector. The range between the upper and lower limits of the curve would decrease if a curved receiver were used; however, the overall accuracy would also become more critical because of the decrease in effective receiver diameter or width.

The curves of Figures 2.6 and 2.7 indicate that if significant optical errors are to be avoided, the reflector of a linear concentrator must be accurate within 0.25° (30:1 concentration ratio) and of a point concentrator within 0.35°-0.5° (over a 200-400:1 concentration ratio range).

2.5 Choice of System Approach

The preceding considerations were evaluated to identify a reasonable system approach for the preliminary baseline system design studies. As a result, a concentrator/receiver system was chosen with the following basic characteristics:

- *Concentrator* — A parabolic dish reflector with a concentration ratio of 400:1.
- *Receiver* — A black body cavity without a transparent quartz radiation shield.

The above system configuration was specified on the basis of the following considerations relative to the other system options:

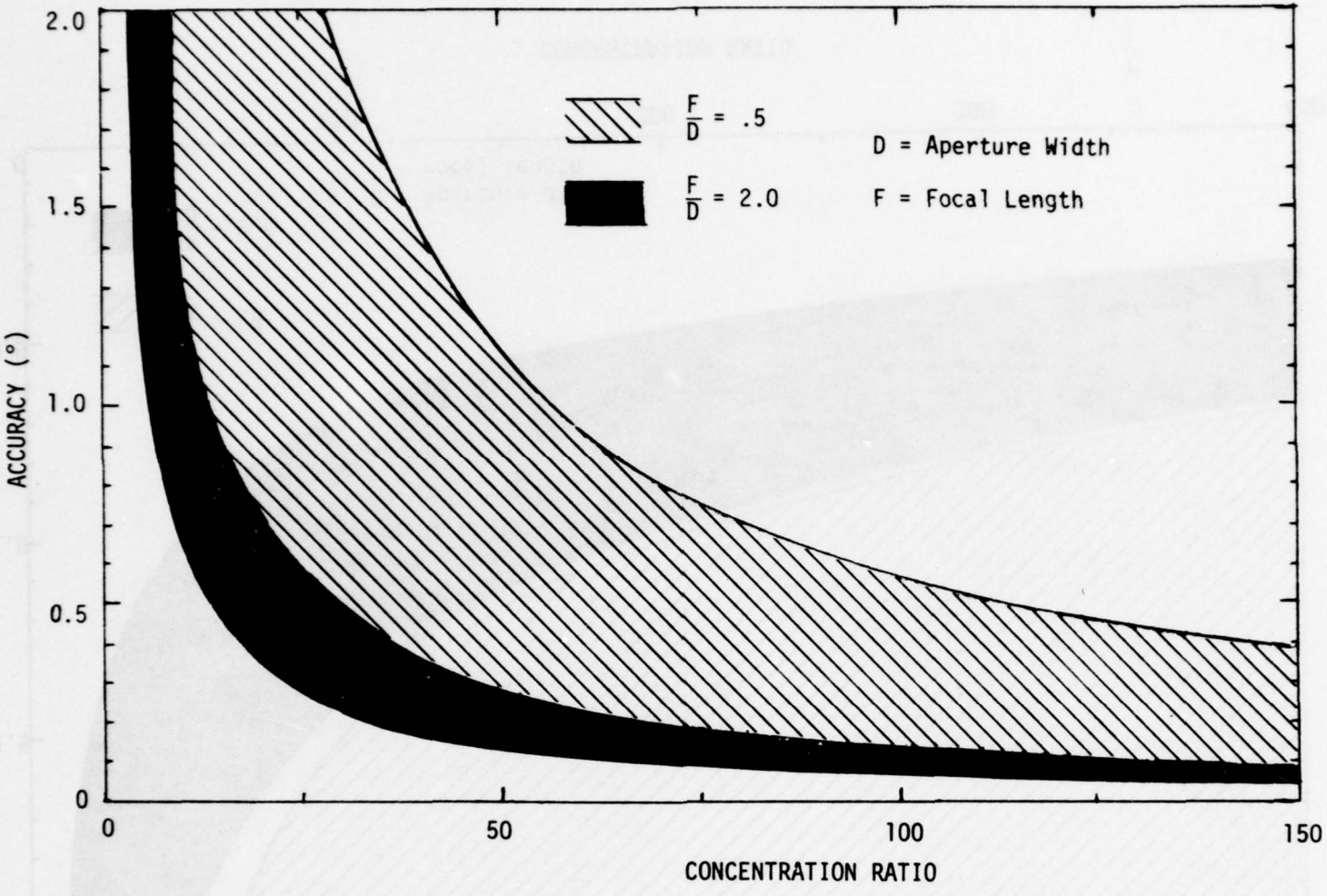

FIGURE 2.6 POINTING/SURFACE ACCURACY FOR PARABOLIC TROUGH CONCENTRATOR

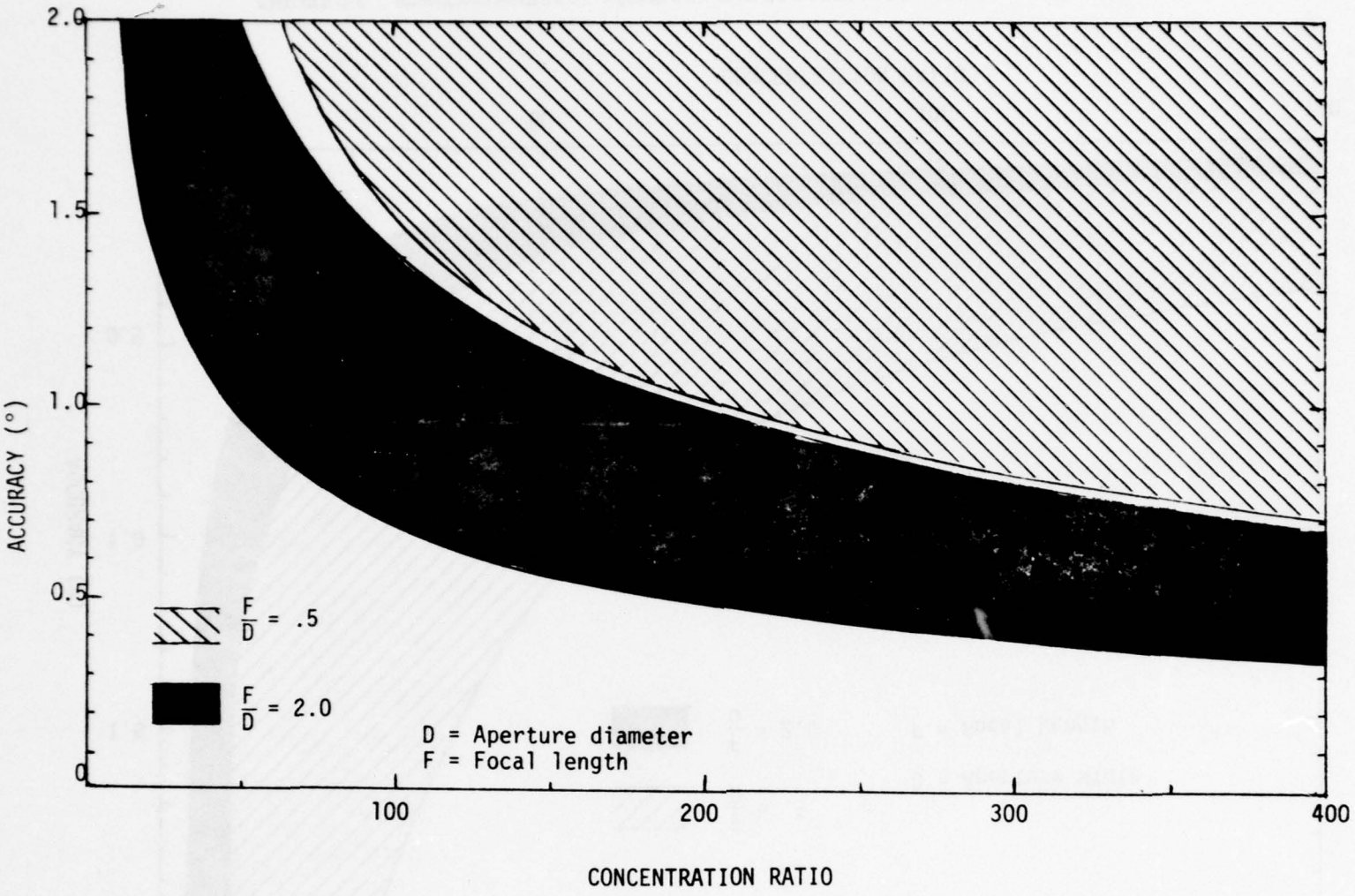

FIGURE 2.7 POINTING/SURFACE ACCURACY FOR PARABOLIC POINT CONCENTRATOR

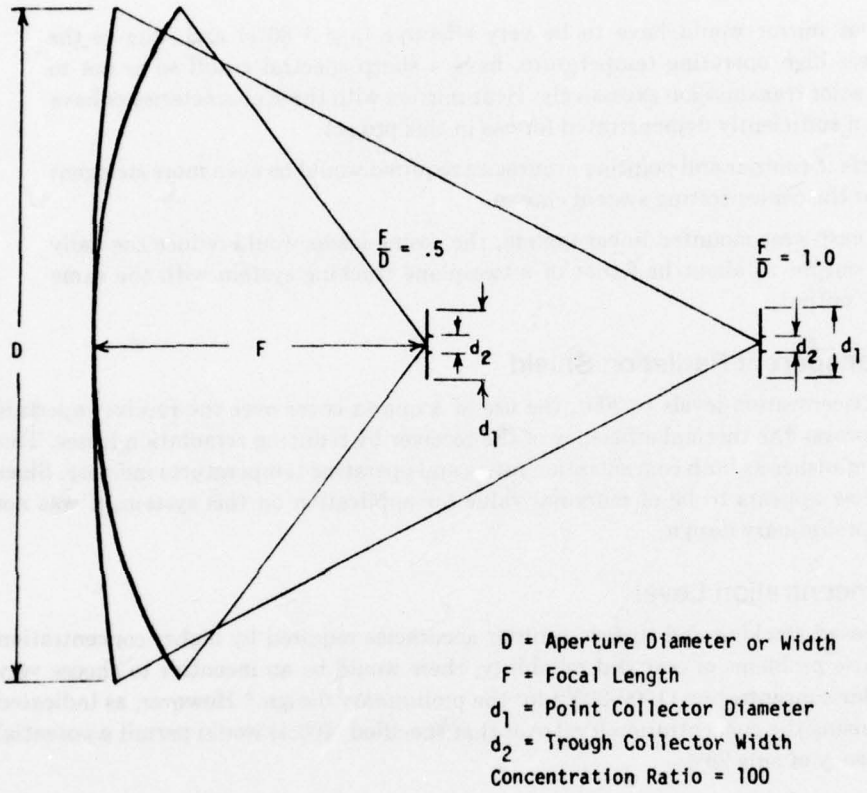

FIGURE 2.8 REPRESENTATION OF POINT/TROUGH COLLECTOR DIMENSIONS

2.5.1 Linear System

A system utilizing a linear concentrator can, in principle, be used if the receiver has an effective heat mirror to greatly reduce reradiation losses. This system was rejected for the following reasons:

- The heat mirror would have to be very effective ($\rho_{IR} > 80\%$) and, due to the relatively high operating temperature, have a sharp spectral cutoff so as not to reduce solar transmission excessively. Heat mirrors with these characteristics have not been sufficiently demonstrated for use in this project.
- The surface contour and pointing accuracies required would be even more stringent than for the concentrating system chosen.
- For an east-west mounted linear system, the cosine losses would reduce the daily energy output to about half that of a two-plane tracking system with the same midday output.

2.5.2 Transparent Radiation Shield

At lower concentration levels (<200), the use of a quartz cover over the receiver aperture significantly improves the thermal efficiency of the receiver by reducing reradiation losses. This improvement diminishes as both concentration ratios and operating temperatures increase. Since the quartz window appears to be of marginal value for application on this system, it was not included in the preliminary design.

2.5.3 Concentration Level

If the increased tracking and surface contour accuracies required by higher concentration levels did not raise problems of cost and reliability, there would be an incentive to choose very high levels of solar concentration (1000-2000) for the preliminary design.* However, as indicated by Figure 2.3, raising the concentration level over that specified (400:1) would permit a potential increase in efficiency of only 20%.

The relatively low concentration ratio chosen was considered to be a "low risk" level which could be achieved with field-erectable mobile equipment. The accuracies required for tracking (~0.25°-0.5°) are consistent with conventional gears and motors. Also, this accuracy should be possible with simple "time clock" control of the tracking mechanism.

The required surface contours would allow for deviations of up to 2 inches over a 15-foot span, which is consistent with reflector segments capable of being erected and dismantled under field conditions.

The indicated system configuration provides a reasonable basis for the design study. Even if future analysis and/or experience indicates that deviations from this design approach are warranted, it is unlikely that these deviations would greatly reduce the overall desirability of the solar-fired open Brayton-cycle engine concept.

*As assumed by some other studies on solar Brayton-cycle engines (References 5 and 6).

2.6 References for Section 2

1. Rabl, Ari, "Comparison of Solar Concentrators," *Solar Energy*, Vol. 18, No. 2, 1976.

2. Jordan, J.F., "Development of Very Low Cost Solar Cells for Terrestrial Use," D.H. Baldwin Co., Cincinnati, Ohio (no date).

3. Fan, J.C., and Bachner, F.J., "Transparent Heat Mirrors for Solar Energy Applications," *Applied Optics*, Vol. 15, No. 4, April 1976.

4. Fan, J.C., et al., "Transparent Heat-Mirror Films of TiO_2/Ag/TiO_2 for Solar Energy Collection and Radiation Insulation, *Applied Physics Letters*, Vol. 25, No. 12, December 1974.

5. Gupta, B.P., "Technical Feasibility of a Modular Dish Solar Electric Systen," Sharing the Sun Conference, August 15-20, 1976, Winnipeg.

6. Jarvinen, P.O., "Windowed Versus Windowless Solar Energy Cavity Receivers," 11th International Energy Conversion Engineering Conference, State Line, Nevada, 1976.

3. SYSTEM PERFORMANCE ESTIMATES AND DESIGN PARAMETERS

3.1 Concentrator/Receiver

The efficiency of the selected concentrator/receiver subsystem is shown in Figure 3.1 for a range of solar radiation levels. A direct insolation level of 275 Btu/hr-ft^2 corresponds to the design conditions and is consistent with that available during the peak daylight hours on a clear day. This curve was used for sizing the baseline system design. (The effect of off-design is discussed in Section 3.5.)

The performance curves of Figure 3.1 were combined with the engine performance characteristics presented in the next section to calculate the overall system performance levels discussed in Section 3.3.

3.2 Engine-Generator

It has been established that the baseline solar energy generator (SEG) system will incorporate an open-Brayton-cycle gas turbine engine driving an alternator. A schematic diagram of this system is shown in Figure 3.2.

In the common fuel-fired version of this cycle, ambient air is compressed, heated by combustion of fuel mixed with the compressed air, expanded to produce shaft power, and exhausted to the atmosphere. A portion of the power from the expander (roughly two thirds) drives the compressor; the remainder is available as output power. In the SEG system, solar heating is substituted for combustion of fuel. The gas-turbine-engine implementation of the Brayton cycle utilizes turbomachinery components — i.e., for the 10-kWe power level, a centrifugal compressor and a radial inflow turbine, mounted on a common shaft.

It is preferable that the engine design be based on an existing unit. A survey of available gas turbine engines (described in Section 4.2) revealed that only one engine with 10-kWe nominal output was in an advanced stage of development. It was developed by the Solar Division of International Harvester (SDIH) for the U.S. Army Mobile Equipment Research and Development Command (USA-MERDC) and is expected to enter production in 1978. This unit and its adaptation to the SEG system are described in Section 4.2.

In the SEG system the solar collector is the major component in terms of size, weight, and cost. The required area of the collector is inversely proportional to the efficiency of the engine-generator set, which provides a strong incentive to select a gas turbine cycle that leads to maximum engine efficiency. The SDIH gas turbine engine (and other small gas turbine units under development) uses a simple open cycle; i.e., no recuperation is provided. However, a cycle with effective recuperation can achieve approximately twice the engine efficiency of the simple cycle at the maximum temperatures of interest, so it would clearly be beneficial to use a recuperator in the SEG system. The cycle projections discussed below are based on a recuperated cycle. The modifications of the SDIH unit to accomplish recuperation are also discussed in Section 4.2.

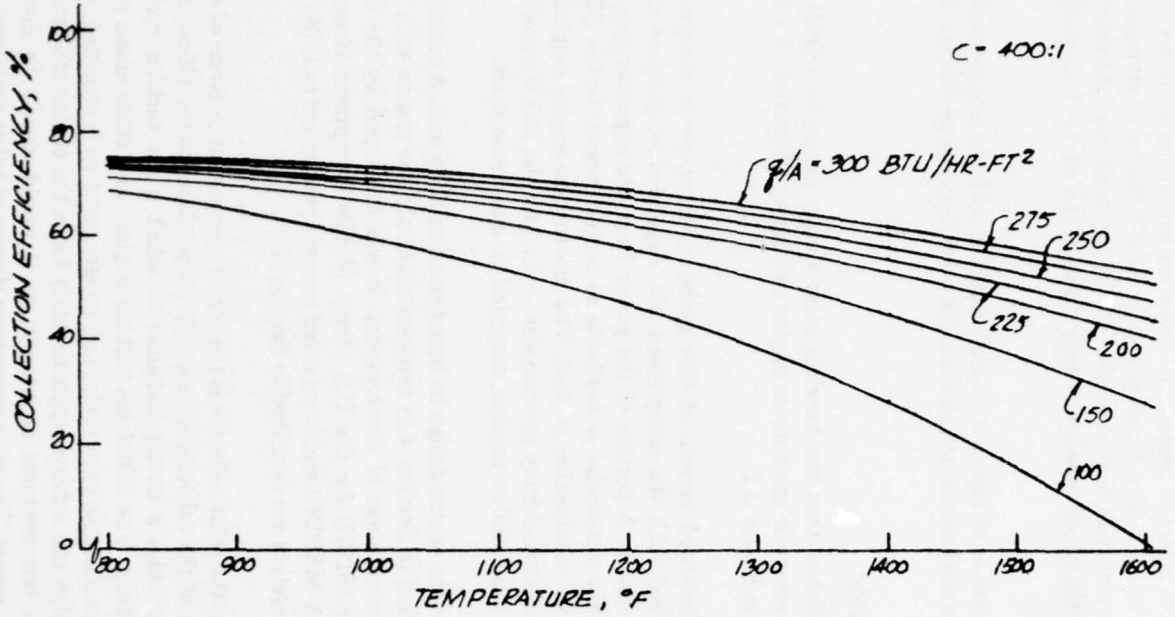

FIGURE 3.1 VARIATION OF CONCENTRATOR/RECEIVER SUBSYSTEM EFFICIENCY WITH SOLAR RADIATION LEVEL

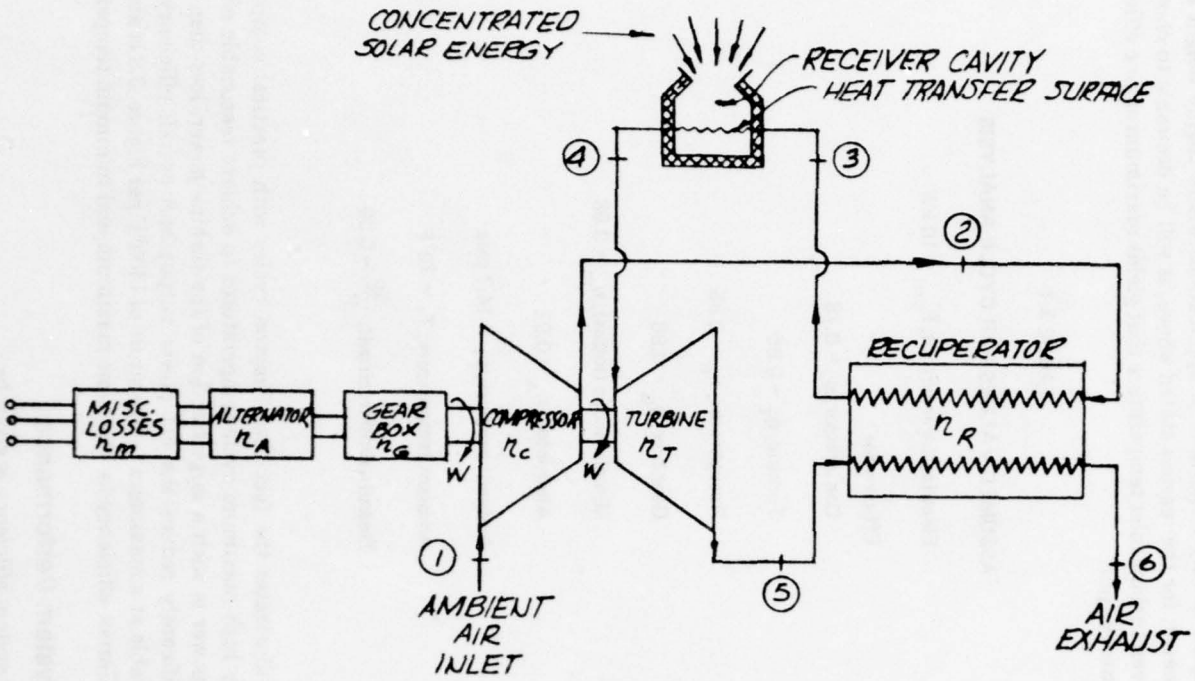

FIGURE 3.2 SOLAR POWERED OPEN-BRAYTON-CYCLE ENGINE: SCHEMATIC FLOW DIAGRAM

The efficiency of an engine-generator set and its specific power output for various turbine inlet pressures and temperatures are shown in Figure 3.3 for the assumed component efficiencies and pressure drops listed in Table 3.1. The indicated efficiency is based on electric power output and includes all generator and gear train losses as well as those associated with the engine itself. High specific power output, which leads to lower air mass flow rate and a smaller engine for a given power output, is very important in applications where engine weight and size are to be minimized. However, for the reasons stated above, it will be desirable to choose a turbine inlet pressure for a given turbine inlet temperature that yields maximum engine efficiency, rather than high specific power output.

TABLE 3.1

ASSUMED VALUES FOR CYCLE ANALYSIS

Electric power output, P_{out} = 10 kW

Efficiencies

Compressor, η_c = 0.78

Turbine, η_T = 0.85

Recuperator, η_R = 0.95

Gear box, η_G = 0.98

Miscellaneous (losses), η_m = 0.98

Alternator, η_A = 0.92

Ambient pressure, p_1 = 14.7 psia

Ambient temperature, T_1 = 70°F

Pressure drop in circuit, $\frac{\Delta p}{p}$ = 0.09

Figure 3.3 illustrates the fact that Brayton cycles with practical component efficiencies require relatively high maximum cycle temperatures to achieve reasonable efficiency. Because the compressor power is such a large fraction of the turbine power, less-than-ideal component efficiencies significantly reduce the net power output and overall efficiency. The maximum efficiency achievable at a maximum temperature of 1400°F per Figure 3.3 is about 30%, which is only 42% of the Carnot efficiency for the same maximum and minimum temperatures.

3.3 Overall System Performance

The overall system efficiency is given by:

$$\eta_s = \eta_{cr} \times \eta_e$$

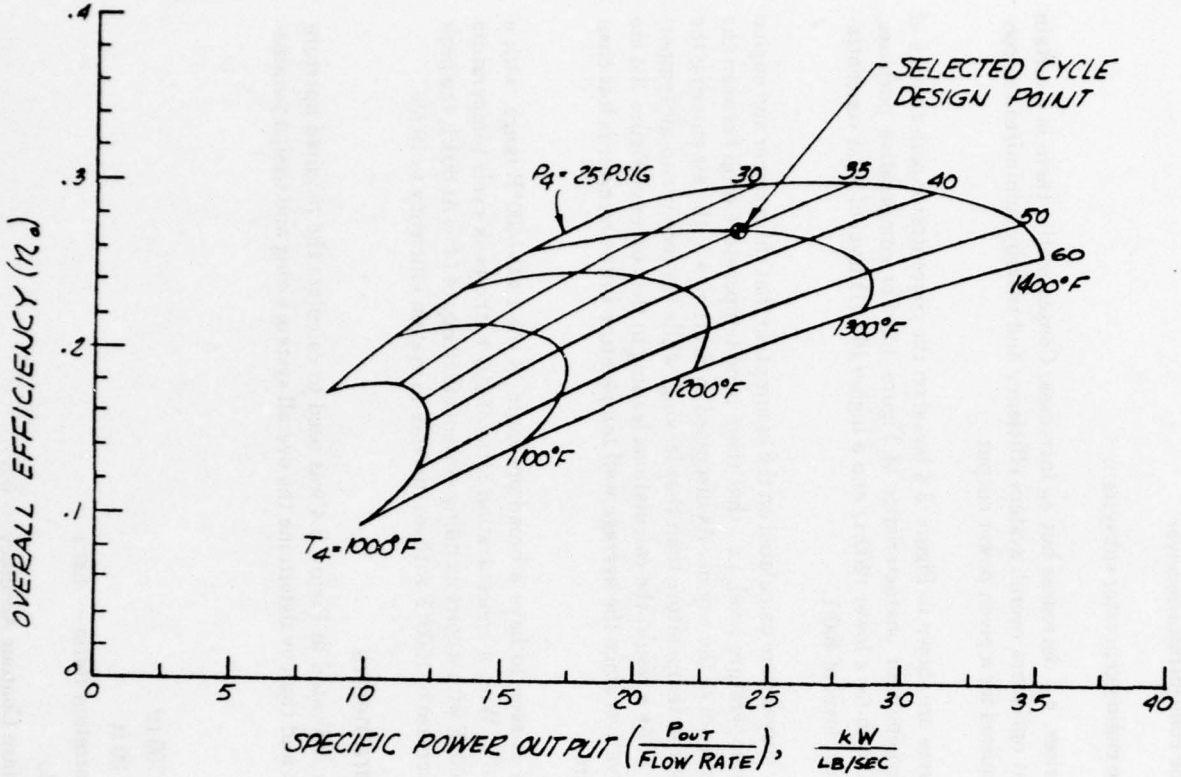

FIGURE 3.3 ENGINE CHARACTERISTICS FOR VARIOUS TURBINE INLET CONDITIONS

where:

η_s = system efficiency, defined as the ratio of electric power output to incident direct solar flux

η_{cr} = efficiency of the concentrator/receiver

η_e = efficiency of the engine/generator subsystem

As the temperature rises, η_{cr} decreases but η_e increases. Consequently, there is a certain operating temperature that optimizes overall system efficiency and thereby minimizes the concentrator aperture area required for a given power output.

System efficiency curves are shown in Figure 3.4 based on the concentrator performance of Figure 3.1 and the engine/generator characteristics of Figure 3.3. For comparative purposes, efficiency curves are also shown for a lower (200:1) and a higher (600:1) level of solar concentration than the assumed design level of 400:1.

The system efficiency curves were calculated on the assumption that the receiver and engine both operate at the same temperature level, i.e., that there is no temperature drop between the receiver walls and the air stream of the engine. As discussed in Section 4.3, the air entering the receiver is about 400°F lower in temperature than that leaving, while the receiver-to-air temperature drops are only 50-70°F. As a result, the calculations leading to the curves of Figure 3.4 are probably somewhat conservative, since the average wall temperature in the receiver is less than the peak engine temperature.

The system efficiency is seen to have a broad optimum in the 1300-1400°F range, with a peak efficiency level of 17.6%. With a concentration ratio of 200:1, the peak cycle temperature would decrease to about 1150°F with a corresponding system efficiency of 14%. At 600:1, the peak cycle temperature would increase to 1500°F with an increase in system efficiency to 19.5%.

3.4 System Design Parameters

The system efficiency indicated in Figure 3.4 was used to calculate the required aperture area for the 10-kWe system and thereby determine the overall system sizing and design parameters listed below.

(a) *Concentrator*

Aperture Area — 705 ft²
Dish Diameter — 30 ft
Geometric Concentration Ratio — 400:1
Reflectivity — 0.85
Tracking and Surface Contour Accuracy — 0.5°
F/D Ratio — 0.6

(b) *Receiver*

Aperture Area — 1.76 ft²
Cavity Diameter — 1.5 ft

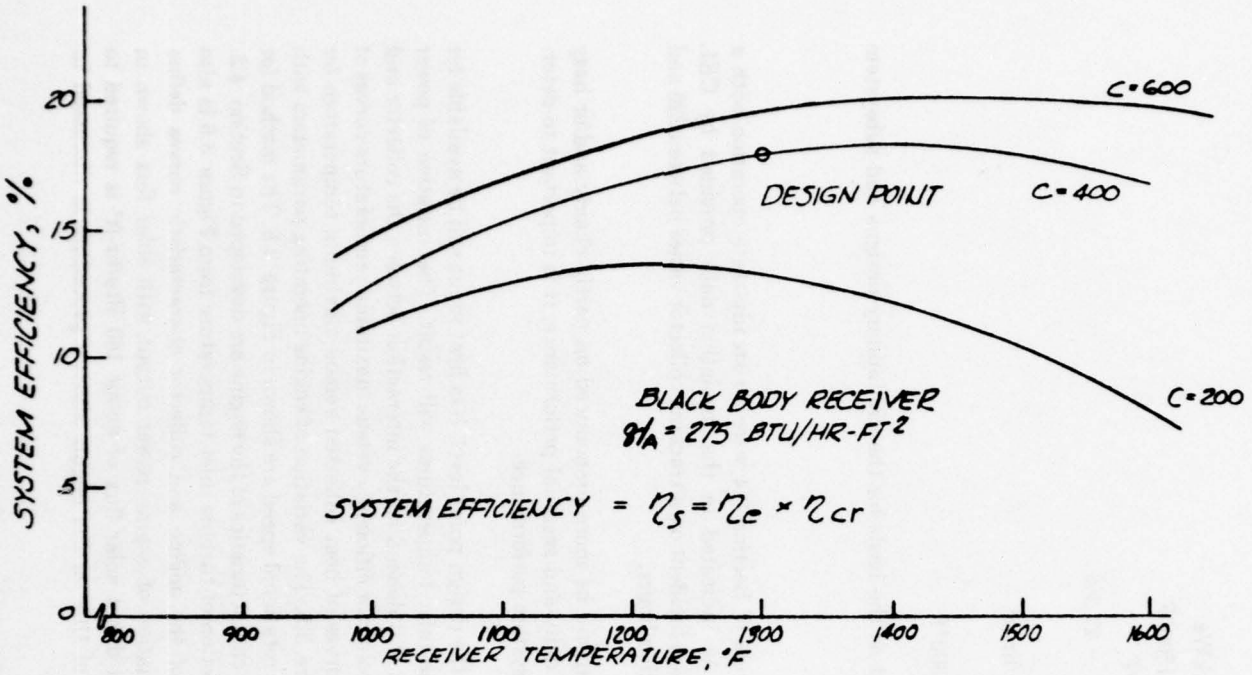

FIGURE 3.4 VARIATION IN SYSTEM EFFICIENCY WITH OPERATING TEMPERATURE

Absorptivity — 0.98

Air Temperature:

Inlet — 980°F

Outlet — 1310°F

(c) *Engine/Generator*

Electric Power Output — 10 kWe

Peak Cycle Temperature — 1300°F

Air Inlet Temperature — 70°F

Engine/Generator Efficiency — 27.3%

(d) *System*

Direct Solar Flux — 275 Btu/hr-ft²

System Efficiency — 17.6%

Operating Temperature — 1300°F

The above parameters were used as the basis for the preliminary designs and subsystem specifications discussed in Section 4.

3.5 Off-Design Operation

The preliminary design parameters of Section 3.4 were for steady-state operation with a direct solar flux of 275 Btu/hr-ft². As indicated in the insolation data provided by CEL (Table 3.2), on a *clear day* the insolation incident on a tracking collector varies between 228 and 288 Btu/hr-ft² during the useful collection hours.

The variation in direct insolation will be more pronounced on partly cloudy and/or hazy days. Therefore, in order to calculate daily and seasonal performance, it is important to determine the effect of direct insolation on system performance.

When the solar flux drops below the design point level, less heat input will be available for the engine air flow, and lower turbine inlet temperatures will result. The variation of power output from the engine with solar flux will depend on the interaction between the collector and engine operating characteristics. The collector efficiency versus maximum temperature curves of Figure 3.1 can be converted to the curves of heat collected versus maximum temperature for various solar flux levels shown in Figure 3.5. The variation of engine operating parameters with turbine inlet temperature for constant rotational speed are shown in Figure 3.6. The method for determining these estimated part-load characteristics of the engine are developed in Section 4.2. The heat input to the engine as a function of turbine inlet temperature from Figure 3.6 is also plotted on Figure 3.5. Intersections of the engine and collector characteristic curves define operating points and lead to the variation of engine power output with solar flux shown in Figure 3.7. As indicated, a minimum direct solar flux of about 180 Btu/hr-ft² is required to initiate engine operation. The effect of this on the engine startup procedure is discussed in Section 4.4.

The variation of engine power output during the day can then be determined, with the result shown in Figure 3.8. To maintain the engine speed constant as the solar flux varies, it will be necessary to vary the load on the generator in accordance with Figure 3.7. The system for accomplishing such load control is discussed in Section 4.4.

TABLE 3.2

CLEAR-DAY INSOLATION LEVELS

t, Solar Time (Hrs from Midnight)	Case I: Latitude = 42° 0′ January 21		Case II: Latitude = 32° 4′ July 21	
	I_{DN}, Direct Normal Insolation (Btu/ft²-hr)	I_d, Diffuse Insolation (Btu/ft²-hr)	I_{DN}, Direct Normal Insolation (Btu/ft²-hr)	I_d, Diffuse Insolation (Btu/ft²-hr)
0	0	0	0	0
1	0	0	0	0
2	0	0	0	0
3	0	0	0	0
4	0	0	0	0
5	0	0	0	0
6	0	0	113.7	12.2
7	0	0	202.9	25.7
8	119.4	5.7	241.3	33.2
9	228.2	15.8	260.8	36.8
10	267.3	17.9	271.5	38.1
11	283.7	19.8	276.8	38.2
12	288.1	20.3	278.5	38.1
13	283.7	19.8	276.8	38.2
14	267.3	17.9	271.5	38.1
15	228.2	13.8	260.8	36.8
16	119.4	5.7	241.3	33.2
17	0	0	202.9	25.7
18	0	0	113.7	12.2
19	0	0	0	0
20	0	0	0	0
21	0	0	0	0
22	0	0	0	0
23	0	0	0	0

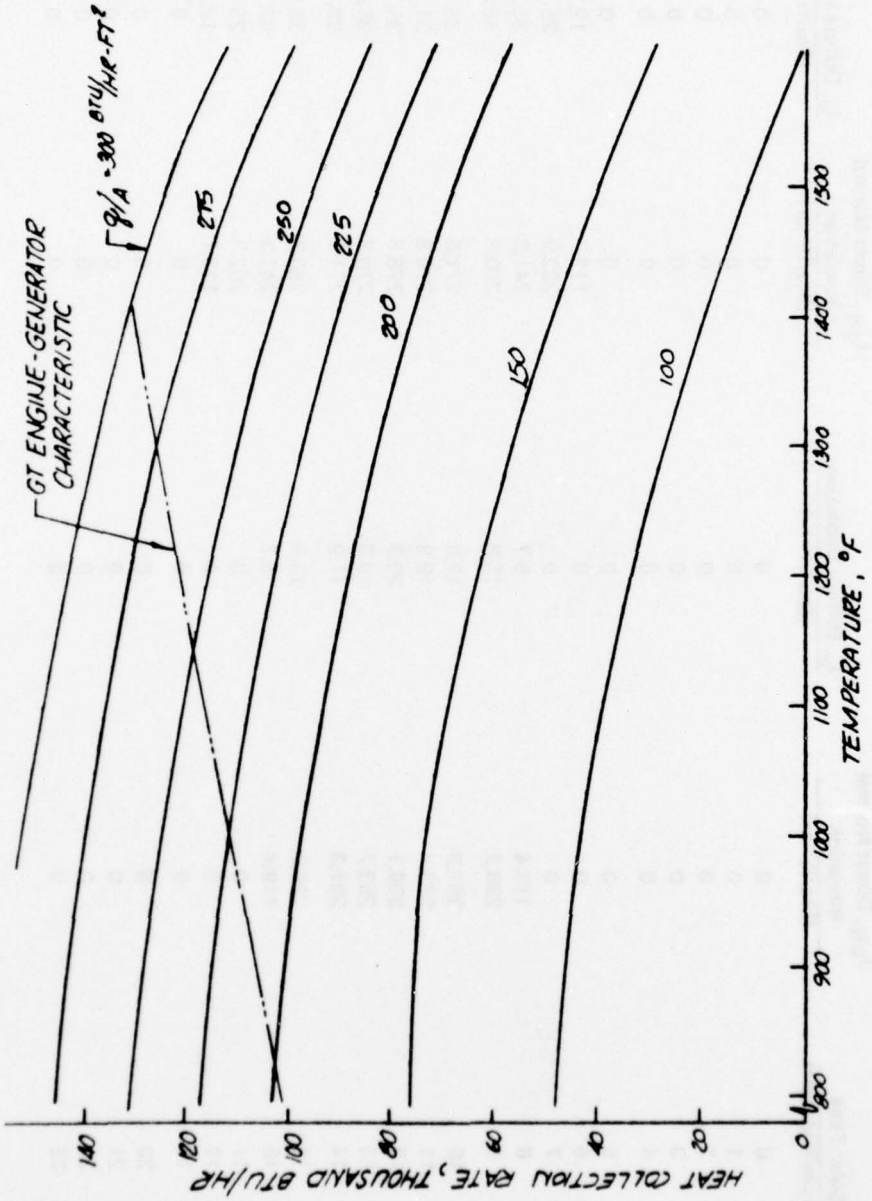

FIGURE 3.5 EFFECT OF INSOLATION ON HEAT COLLECTION RATE

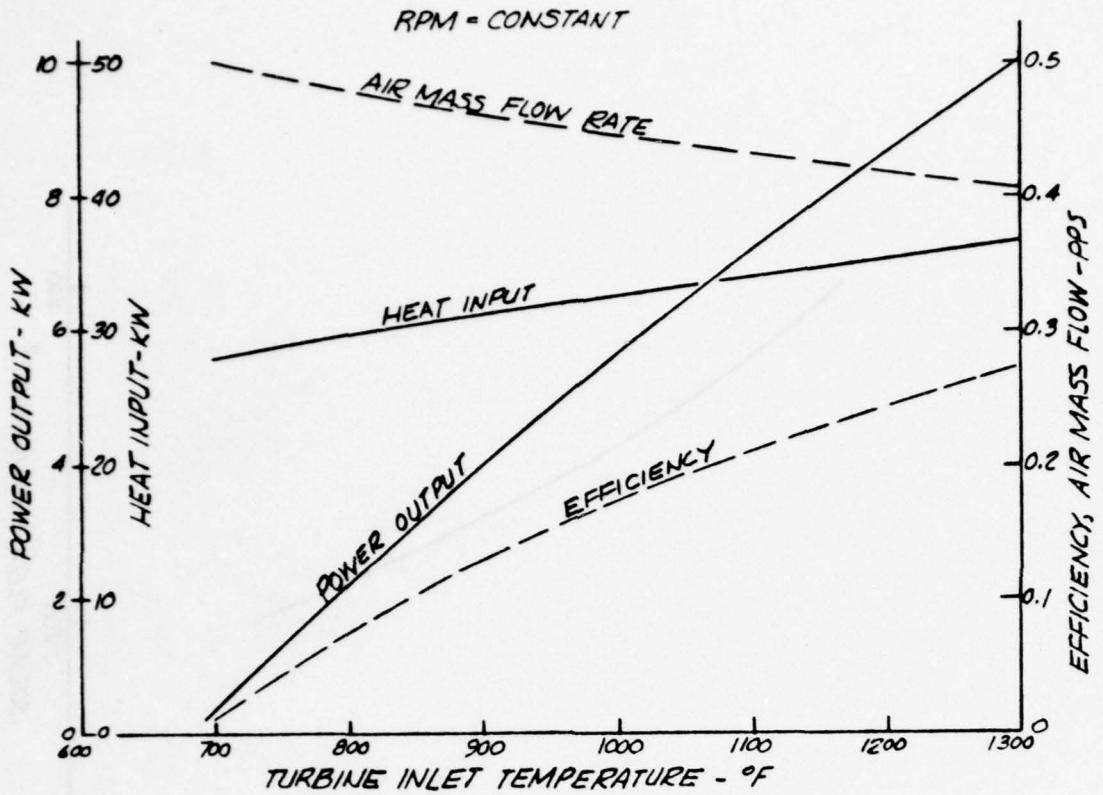

FIGURE 3.6 ESTIMATED ENGINE CHARACTERISTICS AT CONSTANT RPM

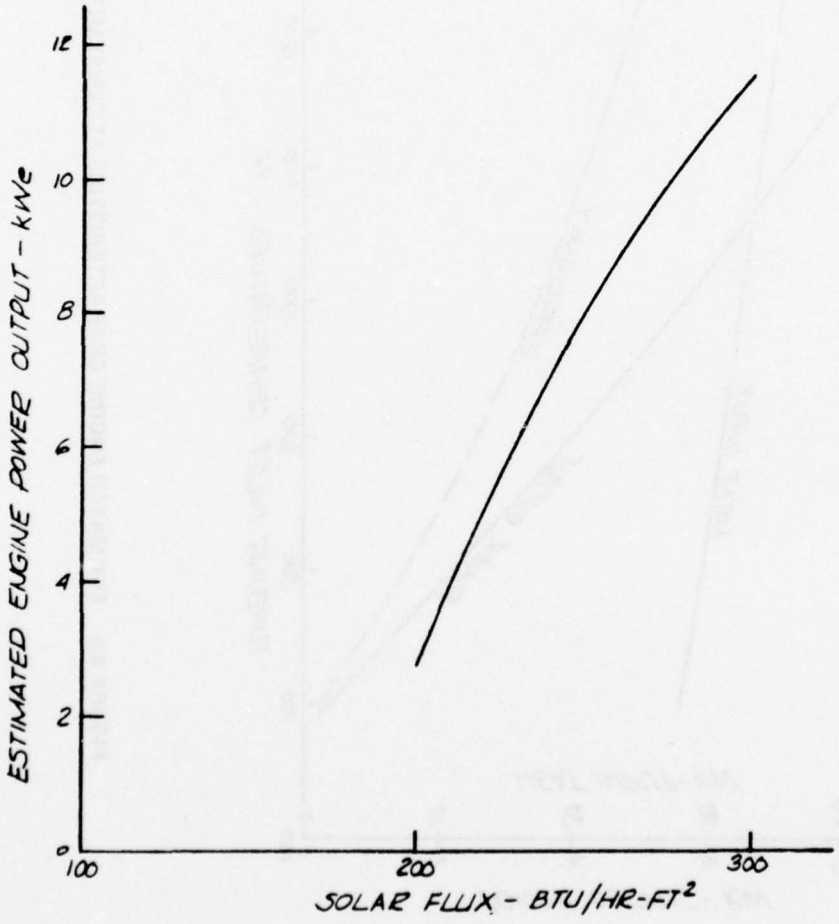

FIGURE 3.7 VARIATION IN SYSTEM OUTPUT WITH SOLAR FLUX

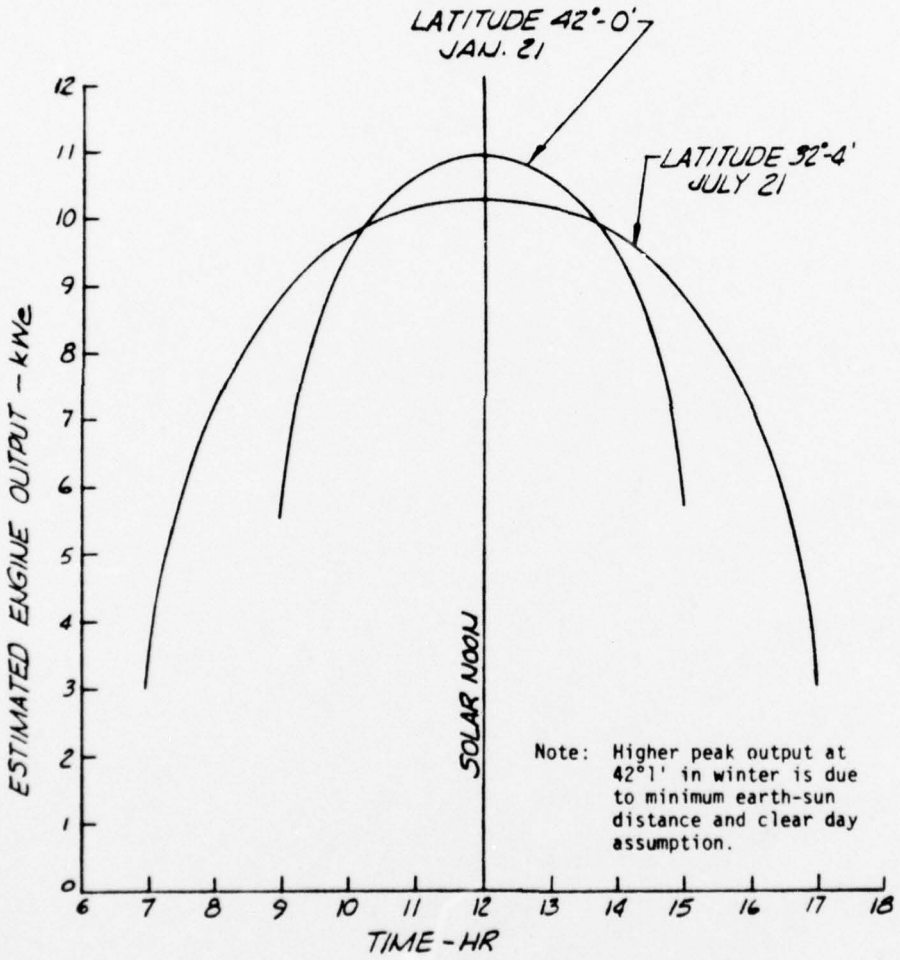

FIGURE 3.8 VARIATION IN ENGINE OUTPUT DURING THE DAY

4. SYSTEM DESIGN

4.1 Concentrator System Design

The major component of the concentration system is the parabolic dish reflector, which must accurately track the sun. The degree of pointing accuracy is determined by the concentration ratio and F/D ratio as indicated earlier (Section 2.4). The tracking system that controls the pointing of the reflector is also a very important part of the solar concentrating system. These two major subsystems comprise the solar concentration system; their design is a critical factor in determining the overall system performance and, more importantly, the cost of the total system.

The following criteria for the design of the concentrating system were generated as a result of considering overall system performance characteristics defined earlier:

- Reflector is approximately 30 feet in diameter.
- Total pointing and surface definition error must be less than 0.7°.
- Surface finish of reflecting surface should be better than 0.4 microinch.
- Reflector structure must be within tolerance when subjected to 25-mph wind loads.
- Reflector assembly should have the capability of being quickly and easily stowed in anticipation of severe wind conditions (greater than 40 mph).
- Concentrator must be segmented and portable for easy assembly, disassembly, and mobility.
- Structure holding receiver should minimize blockage of the sun's energy.
- Distance between receiver and engine should be minimized.
- Cost of design and fabrication should reflect potential production quantities on the order of 1000 systems/year.

The basic construction and operation of the proposed concentrator design are similar to those of equipment already developed and manufactured for the radar and radio astronomy industries. Therefore, manufacturers of large radar antennas were contacted to determine how to approach constructing a large parabolic tracking reflector. Initial contacts included Harris Co. in Melbourne, Florida and Raytheon Company in Wayland, Massachusetts. From discussions with these companies, primarily Raytheon, we were able to identify local manufacturers of large parabolic antennas. Table 4.1 lists the manufacturers we contacted and their related capabilities.

We found that the typical antennas designed and manufactured for the radar industry are produced in limited quantities and are designed for much higher wind loads than would be required for this application. Also, the pointing (tracking) accuracy is often significantly better than this system would require. However, the basic approach to the design of the solar concentrator could be derived from the methods used by the manufacturers of large radar antennas.

TABLE 4.1

SELECTED MANUFACTURERS OF LARGE PARABOLIC RADAR ANTENNAS

Manufacturer	Capability
HARRIS CORPORATION ELECTRONIC SYSTEMS DIVISION Melbourne, Florida	Accurate antenna systems up to 220 feet in diameter for the radar, radio astronomy, and satellite communications applications. Basically special-order systems.
ESSCO West Concord, Massachusetts	Permanent large antenna systems housed in domes, primarily for radio astronomy.
R.F. SYSTEMS, INC. Cohasset, Massachusetts	Permanent and portable large antenna systems for radar, radio astronomy, and satellite systems. Low-cost design approach with some limited production methods.
AINSLIE CORP. Braintree, Massachusetts	Limited design capability. Antennas are primarily one-piece spun construction. Largest made was 20-foot diameter.

4.1.1 Reflector Design

The initial step in designing the reflector is to define its shape. As specified earlier, the shape will take the form of a simple parabola, as defined by the equation:

$$y^2 = 4 F x$$

where:

F = Focal Length

As can be readily seen by the above equation, the focal length determines the shape of the parabola or, for the concentrator system, the shape of the reflector. Data presented in Figure 2.8 gives some indication of the effect of the F/D ratio on the required pointing/surface accuracy of the reflector.

It is desirable to select the F/D ratio which provides the largest error margin allowable for the pointing/surface accuracy. Figure 4.1 presents the allowable accuracy error as a function of the F/D ratio for a concentrator with a concentration ratio of 400. The curve in Figure 4.1 indicates the accuracy required for all reflected energy to be focused within the receiver area as represented by the lower curve of the required accuracy range, as described in Section 2 (Figure 2.8). As indicated by Figure 4.1, the optimum F/D ratio is approximately 0.6, which yields a required total accuracy of greater than 0.7°. Since the overall system performance characteristics, coupled with the requirement for a peak power output from the engine of 10 kW, dictate the aperture diameter (D) of the reflector, the focal length (F) is readily determined and, therefore, the shape of the reflector.

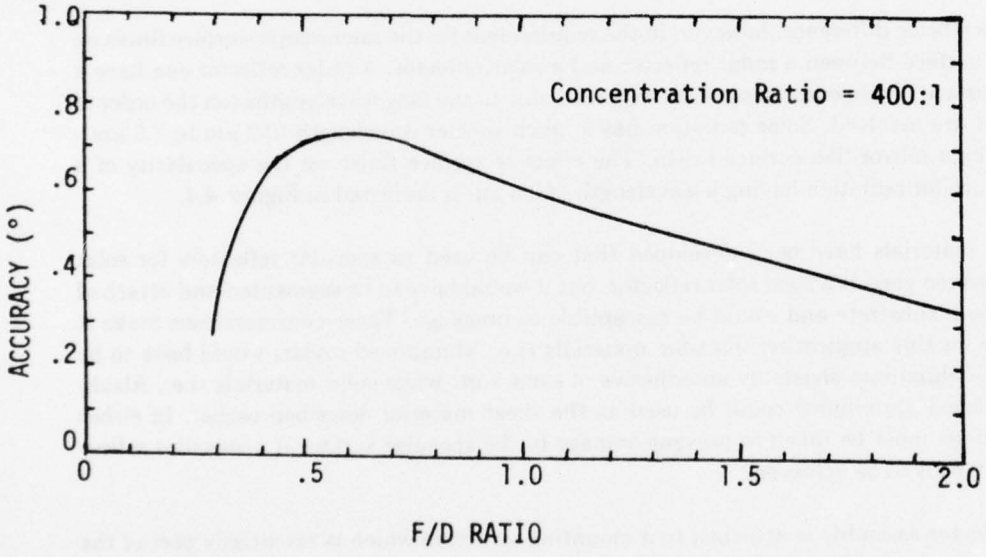

FIGURE 4.1 POINTING/SURFACE ACCURACY AS A FUNCTION OF F/D RATIO

The next step in reflector design is to select the appropriate fabrication method. The construction of the reflector used by three of the antenna manufacturers listed in Table 4.1 is basically the same. The reflector is made of separate individual panels which are made of aluminum sheets bonded or riveted to aluminum channels, as depicted in Figure 4.2. The aluminum sheet is formed to the specified parabolic shape either by hydraulic or mechanical pressure or under vacuum. The sheet is held in this position while the channel structure is attached to the back of the sheet. To allow both the channels and sheets to bend to the required shape without buckling, narrow cuts are made along the edges, as shown in the details of Figure 4.2. Because the material is somewhat elastic, the shape of the pattern used to form the sheets and channels must compensate for this elasticity. This may require several initial modifications to the pattern which will ultimately yield the right shape within the tolerances desired.

The individual panels are then assembled to form a parabolic reflector in the shape desired, as depicted in Figure 4.3. The sections can be made interchangeable to minimize assembly problems and to allow the replacement of individual damaged panels.

There is a basic difference, however, in the requirement for the microscopic surface finish on the reflector surface between a radar reflector and a solar reflector. A radar reflector can have a very rough surface finish, even an open-mesh screen, due to the long wavelengths (on the order of 1 meter) that are involved. Solar radiation has a much shorter wavelength (0.2 μm to 1.5 μm), which requires a mirror-like surface finish. The effect of surface finish on the specularity of a reflector surface for radiation having a wavelength of 0.5 μm is indicated in Figure 4.4.

Several materials have been developed that can be used as specular reflectors for solar radiation. Silvered glass is a good solar reflector, but it would have to be segmented and attached to an aluminum substrate and would be susceptible to breakage. These considerations make it unacceptable for this application. Flexible materials (i.e., aluminized mylar) would have to be applied to the aluminum sheets by an adhesive of some sort, while solid materials (i.e., Alzah, anodized polished aluminum) could be used as the sheet material described earlier. In either case, precautions must be taken to prevent damage to the specular surface if a specular reflectivity goal of 0.85 is to be achieved.

The reflector assembly is attached to a mounting structure which is essentially part of the tracking system, as described in the following section.

4.1.2 Tracking System Design

Two basic types of gimballed mounting systems are used in the radar industry for scanning and tracking satellites. The first is an elevation-over-azimuth type mount, which permits the antenna to move in both elevation and azimuth with essentially no preferred direction of movement. This type of mount is typically used for scanning and tracking many objects or for an antenna that must have the ability to locate and/or track different satellites. The second type is called a polar mount, which primarily moves in a rotational direction about the polar axis of the earth. The movements and adjustments available with a polar mount are indicated schematically in Figure 4.5. It can be seen that the polar mount is ideally suited for tracking the sun, since the sun can be thought of as "moving" in a rotational direction about the earth's spin axis. Current polar mount designs can track satellites with an accuracy of 0.1° with wind speeds of 60 mph, which is well within the requirements for this system. Figure 4.6 shows a conceptual design of the solar concentrator mounting and tracking system, assuming a polar mounting arrangement and including the receiver and Brayton-cycle engine.

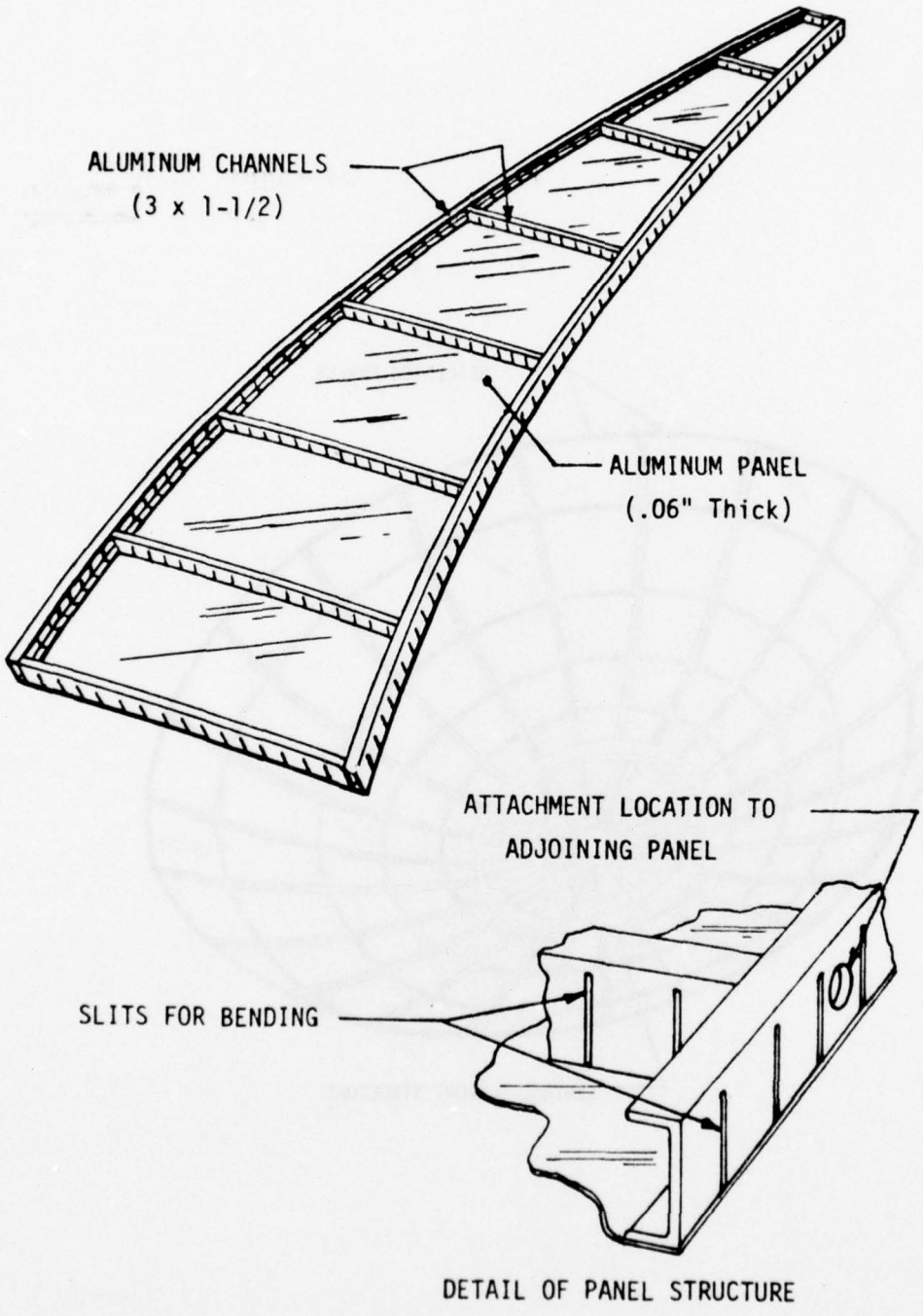

FIGURE 4.2 TYPICAL CONSTRUCTION OF REFLECTOR PANELS

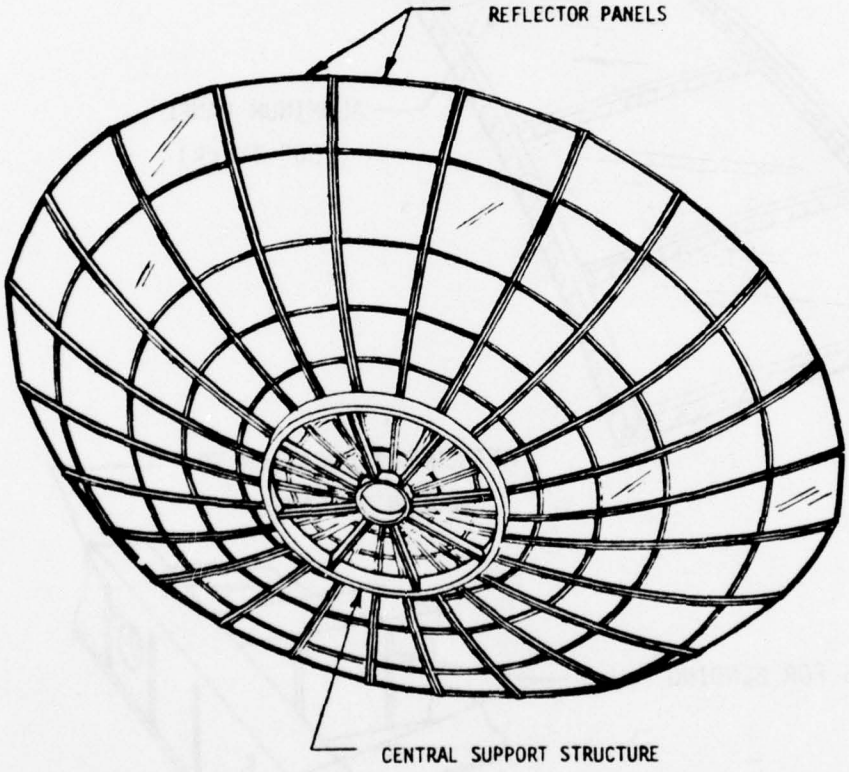

FIGURE 4.3 PARABOLIC REFLECTOR ASSEMBLY

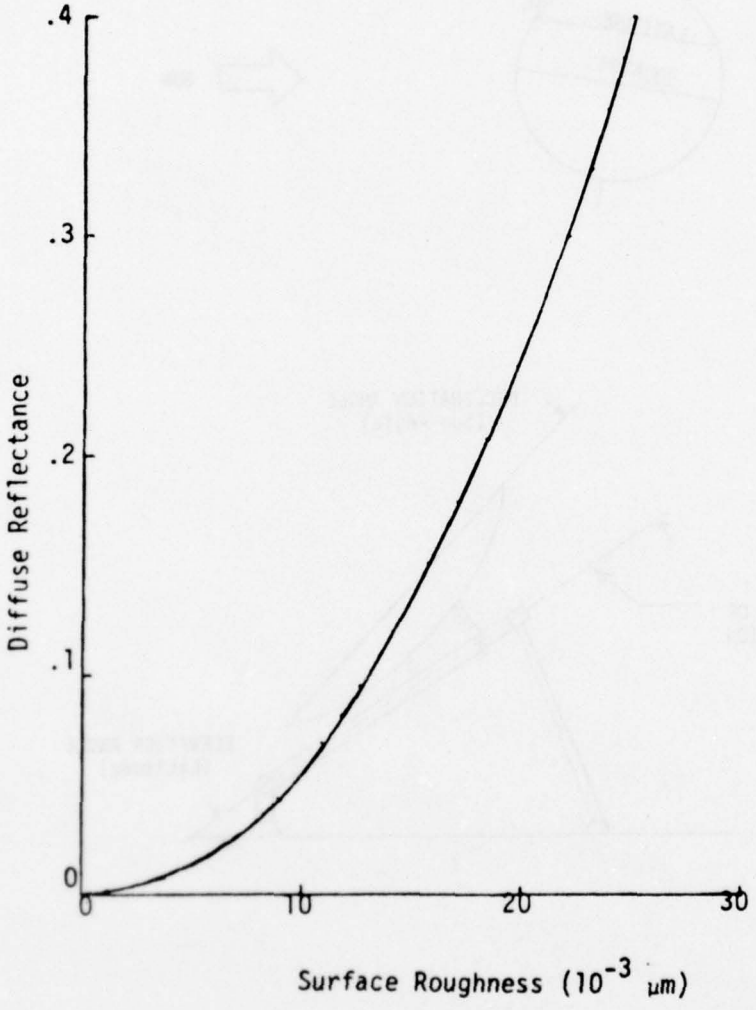

FIGURE 4.4 DIFFUSE REFLECTANCE OF SOLAR ENERGY ($\bar{\lambda}$ = .5 μm) AS A FUNCTION OF SURFACE FINISH (RMS)

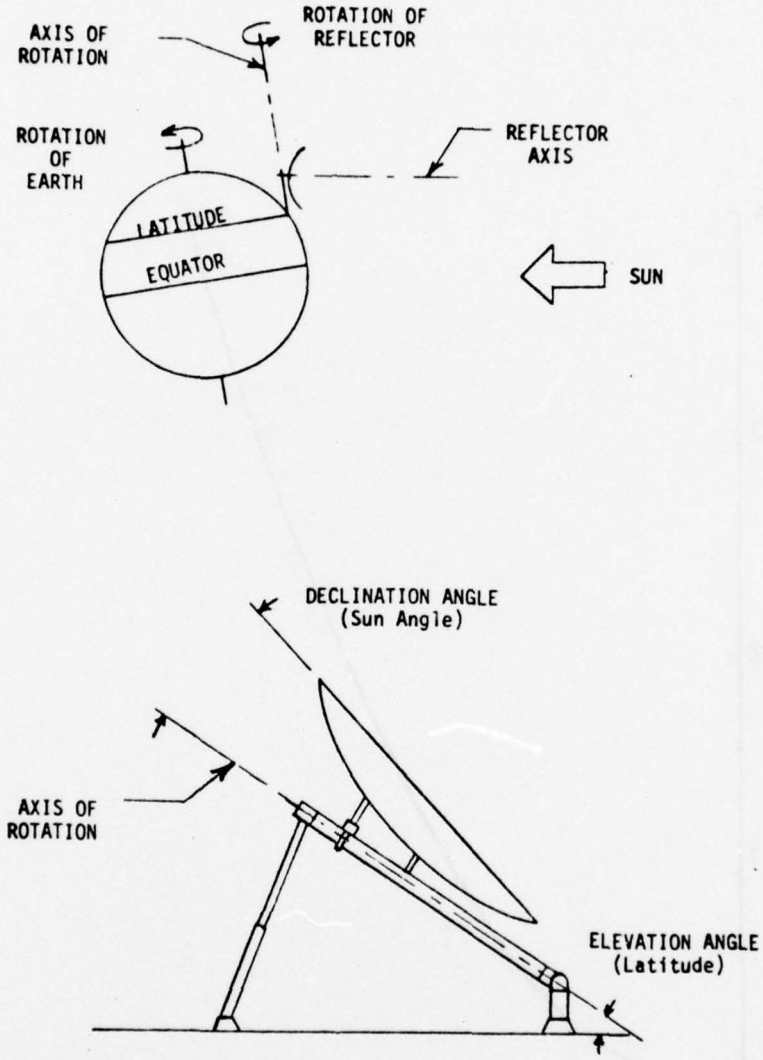

FIGURE 4.5 PRINCIPLE OF OPERATION OF A POLAR MOUNTING SYSTEM

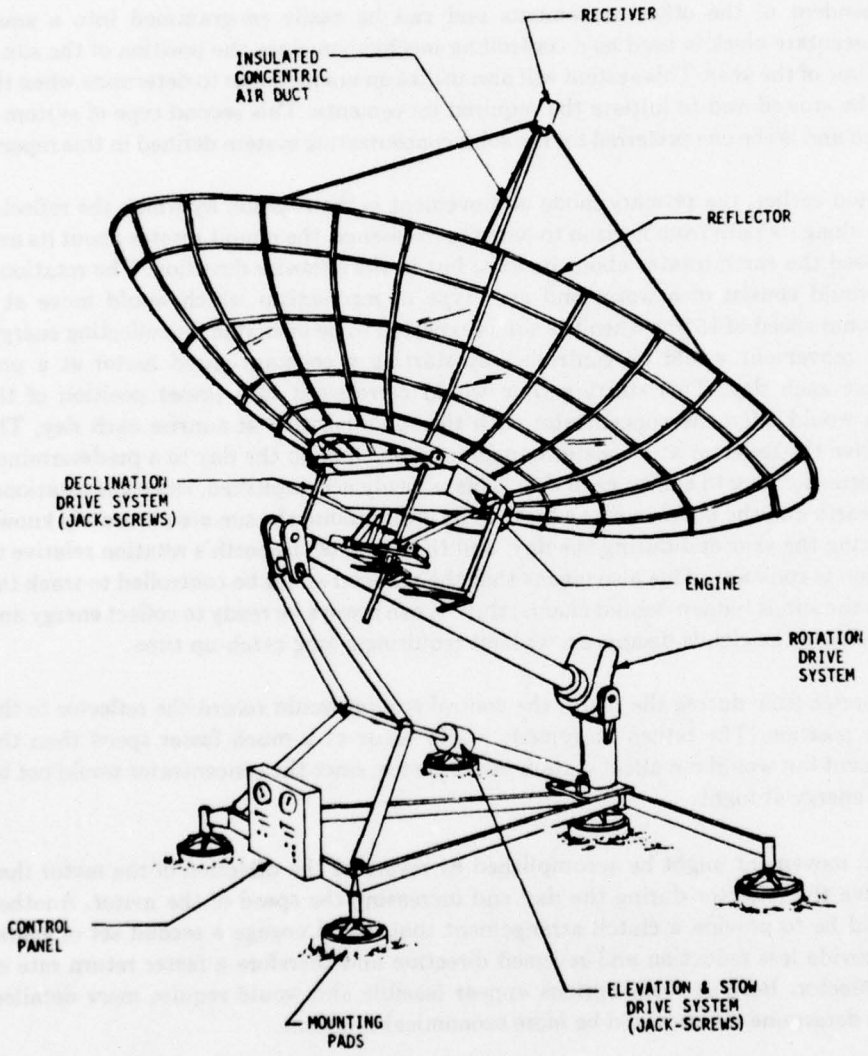

FIGURE 4.6 CONCEPTUAL DESIGN FOR 10-kW SOLAR CONCENTRATOR SYSTEM

There are basically two options available for the system logic that controls the movement of the tracking system. One is a closed feedback loop which senses the position of the sun and corrects the position of the concentrator to point in the direction of maximum solar energy. With this type of logic, the system is continually correcting the position of the reflector. There is also a problem when the sun goes behind the clouds, in that the system may take a significant period of time to realign the concentrator with the sun when it reappears. Another type of system is one which utilizes a small clock-controlled "computer." This type of system logic is more suited to a polar-type tracking system, in that each direction of movement of the polar mount, as described later, is independent of the other movements and can be easily programmed into a small computer. An accurate clock is used as a controlling mechanism since the position of the sun is known at any time of the year. This system will also utilize an anemometer to determine when the reflector must be stowed and to initiate the required movements. This second type of system is less complicated and is the one preferred for the solar concentrating system defined in this report.

As indicated earlier, the primary mode of movement is the rotation by which the reflector follows the sun along its path from horizon to horizon; in essence, the mount rotates about its axis at the same speed the earth rotates about its axis, but in the opposite direction. The rotational drive system would consist of a worm and gear type of mechanism which would move at a constant rotational speed of 15°/hr when the sun is expected to be available for collecting energy. The rotational movement would be controlled by starting a constant-speed motor at a predetermined time each day. This starting time would correspond to a preset position of the reflector which would align the concentrator with the sun's position at sunrise each day. The motor would drive the reflector at a constant angular speed through the day to a predetermined stop position corresponding to sunset each day. This is easily accomplished, since the rotational position of the earth and the position of the earth in its orbit around the sun are accurately known at any time during the year and during the day, and the speed of the earth's rotation relative to the sun's position is constant. This also means that the reflector could be controlled to track the sun, even when the sun is hidden behind clouds; thus, it can always be ready to collect energy and provide power should the clouds disappear, without requiring a long catch-up time.

At some preset time during the night, the control system would return the reflector to the start or sunrise position. The return movement would occur at a much faster speed than the tracking movement but would not affect system performance, since the concentrator would not be collecting solar energy at night.

The return movement might be accomplished by reversing the direction of the motor that was used to drive the reflector during the day and increasing the speed of the motor. Another possibility would be to provide a clutch arrangement that would engage a second set of gears. These would provide less reduction and reversed direction and therefore a faster return rate of travel of the reflector. Both of these options appear feasible and would require more detailed investigation to determine which would be more economical to utilize.

A second mode of movement is in the declination angle of the reflector relative to the polar axis of the mount. Again, the declination of the sun with respect to the polar axis of the earth is accurately known throughout the year. This angle is determined by the time of year; i.e., at summer and winter solstices, the declination angle is up 23.5° and down 23.5°, respectively, and at vernal and autumnal equinoxes, the declination angle is 0°. Any adjustments in this angle can

be made when the reflector is not tracking the sun; i.e., at night. The maximum change of angular declination of the sun during a 12-hour period occurs at equinox. This total movement is 0.25°, which is well within the total accuracy tolerance for the pointing system.

The adjustment of the declination angle in a typical radar system is made using a jack-screw mechanism, which is felt to provide the accuracy required without undue expense. This adjustment could be controlled by a stepping motor which drives the jack-screw mechanism. The amount of movement in the declination angle would vary from no movement at the solstices to approximately 0.5°/day at the equinoxes. The amount of movement each time the stepping motor is invoked would be recorded, possibly by an encoder, to determine if the reflector is at the correct angle of declination throughout the year. This is to ensure that an unforeseen random error does not occur in the control system which drives the stepping motor. Such an error might result in an incorrect number of pulses being issued to the stepping motor, which could put the reflector permanently out of alignment.

The third mode of movement is the elevation angle of the polar mount itself. The elevation of the mount would be mechanically set at the time of erection of the solar concentrating system and would be dependent only on the latitude of the site. The only movement that would occur in the angle of elevation would be under adverse wind conditions, at which time the control system would issue a command to stow the reflector. This would be accomplished by driving a jack-screw mechanism attached to a collapsing tripod, as indicated in Figure 4.6, which would lower the reflector to a horizontal position and would also return it to its operation position. As the polar mount is lowered, the reflector would have to be moved to a noon-time position to avoid hitting the ground when the mount is in the fully stowed position. This could be accomplished by using the rotational drive motor in a fast mode of operation, if possible, or by disengaging the rotational drive motor and mechanically moving the reflector to a noon-time position with a lever-arm type of mechanism. Again, the option chosen would depend on the more economical system.

The stow mode of operation would only be initiated if sustained wind speeds of over 25 mph were measured for a predetermined period of time, or an instantaneous wind speed of 45 mph were recorded. It is expected that the high-wind condition that would effect a stowage of the reflector would indicate weather conditions not conducive to effective operation of the SEG unit. Therefore, to avoid a continual up-and-down movement of the reflector mount and to simplify the control system, the control system would be automatically reset and would not return to normal operation until the beginning of the next day. However, there would be the capability of manually resetting the system, which would cause the system to return to normal continued operation after a brief restoration period during which the system realigned itself with the sun.

4.1.3 Weight Breakdown

An important design consideration which affects the type of construction of the reflector and the materials chosen is the requirement that the system be portable. This suggests that the total weight and compactness of the system is important. Since the wind load and accuracy requirements are less stringent for the solar concentrator system than for typical radar antenna systems, the reflector and support structure can use a less rigid and, therefore, less massive structure. The resulting weights of the various concentrator system components are listed in Table 4.2.

The reflector panels were assumed to be made from 3 x $1\frac{1}{2}$ x $1\frac{5}{8}$ inch aluminum U-channels, which were used for both the longitudinal and radial support members, and .06-inch

TABLE 4.2

WEIGHT BREAKDOWN OF CONCENTRATOR SYSTEM COMPONENTS

Component	Weight (lb)
REFLECTOR	
– Panels (24 @ 117 lb)	2,808
– Support Ring	240
POLAR MOUNT	
– Central Shaft with Reflector Support System	1,050
– Drive System	500
– Elevation Support and Drive System	450
SUPPORT FRAME	
With Associated Systems	1,500
Total	6,548

sheet aluminum. The resulting weight of each panel is 117 lb, which can be easily handled by two or three men. The central support ring was considered to be made of 6 x 2 inch aluminum box members.

The central shaft of the polar mount was assumed to be made of a 15-foot long hollow cylinder, made of stainless steel, having an outside diameter of 12 inches and a wall thickness of 1 inch. This construction was determined to be sufficient to hold the reflector to within an accuracy of 0.1° of rotational movement under maximum load.

The support frame for the total system was assumed to be made of structural steel with sufficient cross-section to maintain the rigidity desired for the concentrating system.

The weight of the drive system was determined from existing data on current systems manufactured by R.F. Systems, Inc. The weight of the rotational drive system is primarily determined by the gear reduction system that is needed. Typical motors used for these systems run at a speed of 1750 rpm. This must be reduced to .0007 rpm, which requires a large gear reduction system.

The total weight of the concentrator system, which is the major weight component of the total solar-powered system, has been estimated to be approximately 6500 pounds. The sizing of the structural members is somewhat conservative, and a significant weight reduction from that indicated above could probably be achieved with a greater design effort. As indicated in Section 4.4, the above weight is consistent with the overall program goals.

4.2 Engine-Generator Set

4.2.1 Survey of Available Engines

All companies in the United States known to be active in small gas turbine technology were contacted to determine what engine-generator systems or components might be available for the

TABLE 4.3

SUMMARY OF INFORMATION FROM CONTACTS WITH COMPANIES ACTIVE IN SMALL GAS TURBINE TECHNOLOGY

Company	Unit Closest to 10-kWe Requirement	Development Status	Remarks
Solar Division of International Harvester	10-kWe Generator Set, Model MEP-412A (Developed for USA-MERDC)	22 units built or in manufacture. 6,000 hours operating time accrued	Non-recuperated cycle
AiResearch Division of Garrett Corporation	30-kWe Generator Set, Model GTGE 36-2 (Developed for USA-MERDC)	Prototype now under endurance test.	Non-recuperated cycle
Williams Research Corporation	56-kW engine	Prototype (3)	Regenerative cycle
Energy Transformation Corporation	None directly applicable	–	Focus has been on low cost and maintenance, not on high efficiency
Northern Research Corporation	Do not mfr. engines Do R&D for clients	–	–
Eaton Corporation, Research Ctr.	11-35 kW engines for recreational vehicles	Prototype developed	Non-recuperated cycle Data are proprietary

The Solar Division of International Harvester Company is developing the new general purpose 10 KW, 60 Hz gas turbine generator set for the United States Army Mobility Equipment Research and Development Center, Fort Belvoir, Virginia.

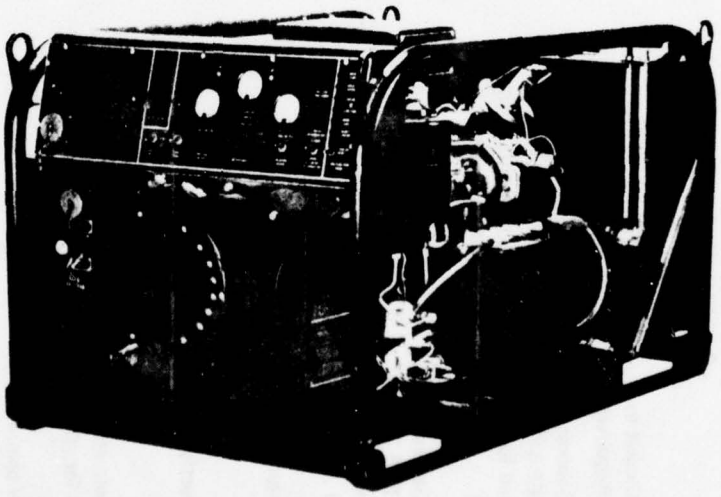

FIGURE 4.7 SOLAR: 10-kW, 60Hz GAS TURBINE GENERATOR SET

A new, lightweight, rugged, highly reliable gas turbine engine for application in generator sets, mechanical drive packages, or auxiliary power units for ground-cart use. It is designed to meet all military requirements while preserving low-cost production concepts.

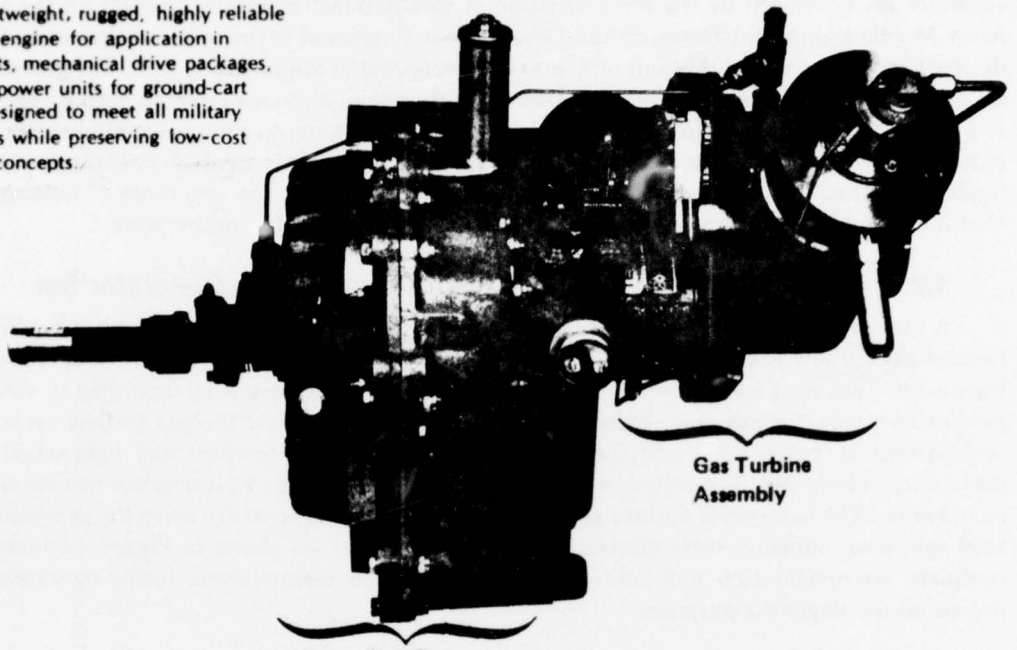

General Characteristics

Fuel
MIL-J-5624, JP-4 and -5, MIL-F-16884 VV-F-800, Diesel DF-1 and DF-2, MIL-G-3056, AVGAS

Oil
MIL-L-2104, MIL-L-7808, MIL-L-10295

Output Pad Speed
3600 or 4000 rpm

Rotor Speed
93,500 rpm

Rating
28 horsepower

Ambient Conditions
59°F at sea level

Fuel Consumption
29 pounds/hour

Accessory Drive
Two-Pad

Weight
95 pounds

Time Between Overhaul
6000 hours

Engine Air Flow
0.40 pounds/second

Mean Time Between Failure
790 hours

Operating Environment
Temperature -65°F to +130°F

Altitude
Sea level to 8000 feet

FIGURE 4.8 SOLAR: GAS TURBINE ENGINE-MODEL T-20G-1

baseline SEG system. The results of our inquiries are summarized in Table 4.3. The engine-generator set developed by the Solar Division of International Harvester (SDIH) for the U.S. Army Mobile Equipment Research and Development Command is the only existing unit of the desired size. Production of this unit for the Army is expected to commence in 1978. The generator-set developed by AiResearch Division of Garrett Corporation, although larger in output than the 10 kW level, is close enough in size to provide relevant information on component efficiencies and part-load performance. AiResearch has also developed closed-cycle gas turbines using working fluids other than air (e.g., argon, helium-xenon mixtures, etc.) in the size range of interest.(1) Useful information on component efficiencies has also been derived from this work.

4.2.2 Description of the Fuel-Fired SDIH Gas Turbine Generator Set

A view of the generator set is shown in Figure 4.7. The generator set incorporates the SDIH Gemini gas turbine engine, Model T-20G-1; its characteristics are shown in the data sheets of Figure 4.8. Technical features and the development of the unit have been described in various publications (see, for example, Reference 2). Salient parameters for the gas turbine cycle are summarized in Table 4.4. Since the unit was developed to be compact and lightweight for portability in field use, it operates on the simple gas-turbine cycle, i.e., it does not incorporate a recuperator. The high-speed turbine shaft operates through a gear box to drive the generator at 3600 rpm for producing 60-Hz electric power. The generator set shown in Figure 4.7 includes complete instrumentation and controls for operation and maintenance, including extensive provisions for diagnostic purposes.

TABLE 4.4

CYCLE PARAMETERS, SDIH GEMINI ENGINE(2)

Pressure Ratio	3.42
Compressor Efficiency	0.753
Compressor Airflow, pps	0.452
Turbine Inlet Temperature, °F	1310
Turbine Efficiency	0.825
Turbine Exhaust Temperature, °F	935
Shaft Power Output, kW	15.1

4.2.3 Gas Turbine Engine Generator Set for the SEG System

As noted in Section 3, the recuperatored cycle is preferred for the SEG system because it makes the engine approximately twice as efficient as with the simple cycle. It was also shown in Section 3 that a turbine inlet temperature of about 1300°F and an inlet pressure of 35 psia led to optimum efficiency for the engine-generator set (Figure 3.3) and also to best overall efficiency for the combined collector-receiver/engine-generator system (Figure 3.4). Other parameters for the recuperated gas-turbine cycle corresponding to these turbine inlet conditions are summarized in Table 4.5.

TABLE 4.5

SUMMARY OF PARAMETERS FOR SELECTED GAS TURBINE CYCLE

Electric Power Output, P_{out} = 10 kW

Efficiencies

Compressor, η_c = 0.78

Turbine, η_T = 0.85

Recuperator, η_R = 0.95

Gear Box, η_G = 0.98

Miscellaneous (losses), η_m = 0.98

Alternator, η_A = 0.92

System Data

Pressure Drop in Circuit, $\frac{\Delta p}{p}$ = 0.09

Air Mass Flow Rate, w = 0.407 pps

Cycle efficiency, η_{cy} = 0.309 (neglecting η_G, η_m and η_A)

Overall Efficiency, η_o = 0.273

Heat Input at Collector = 85.3 Btu/lb

Compressor Work = 49.1 Btu/lb

Turbine Work = 75.5 Btu/lb

Pressures/Temperatures

Location*	Pressure-psia	Temperature °F
1	14.7	70
2	36.8	274
3	36.4	981
4	35.0	1,300
5	15.3	1,018
6	14.7	311

*Refer to Schematic Flow Diagram, Figure 3-2.

The pressure ratio for the SEG system engine is lower than that for the SDIH unit because the optimum pressure ratio for a recuperated cycle is lower than that for a simple cycle. Reduced pressure ratio means that somewhat lower tip speeds can be used for both the compressor and the turbine. Lower tip speeds can be accomplished by lower rotational speed, smaller wheel diameters or a combination of the two, the choice being made so as to achieve best component efficiencies. Using the correlations for component efficiency as a function of design parameters developed by Balje,[3] we have projected the compressor and turbine characteristics for the recuperated cycle summarized in Table 4.6. In making these projections, we have sought a balance in optimizing both compressor and turbine efficiency. The wheel diameters and the flow rates of the recuperated engine are very similar to those of the SDIH unit. Hence, the two engines would be about the same size. The compressor and turbine efficiencies shown in Table 4.6 are somewhat higher than those for the SDIH unit for several reasons:

TABLE 4.6

PROJECTED COMPRESSOR/TURBINE CHARACTERISTICS FOR THE RECUPERATED CYCLE

	Compressor	Turbine
Specific Speed*	85	75
Specific Diameter*	1.76	1.32
Tip Speed, fps	1,350	1,260
Rotational Speed, rpm	81,390	81,390
Wheel Diameter, in.	3.81	3.56
Efficiency	0.78	0.85

*Per Balje's definitions (Reference 3).

1. The specific speed of the compressor for the recuperated engine (85) is higher than that of the SDIH unit (about 76), so a somewhat higher compressor efficiency may be achievable.
2. The lower pressure ratio of the recuperated cycle should lead to reduced internal air leakage from high-pressure to low-pressure regions; reduced leakage losses can be considered as equivalent to improved compressor/turbine efficiencies.
3. The design and aerodynamic development of the compressor and turbine for the SDIH engine occurred between 1965 and 1970. Somewhat higher component efficiencies might be achieved in a future development of new components. Higher component efficiencies have been reported for other units of this size.[1]

The recuperator effectiveness of 0.95 shown in Table 4.5 is higher than values that typically result from optimization studies directed at minimizing the cost of power for fuel-fired systems.[4] It was chosen because in the SEG system there is a direct tradeoff between recuperator effectiveness and solar collector size. This tradeoff is indicated by Figure 4.9, which shows overall

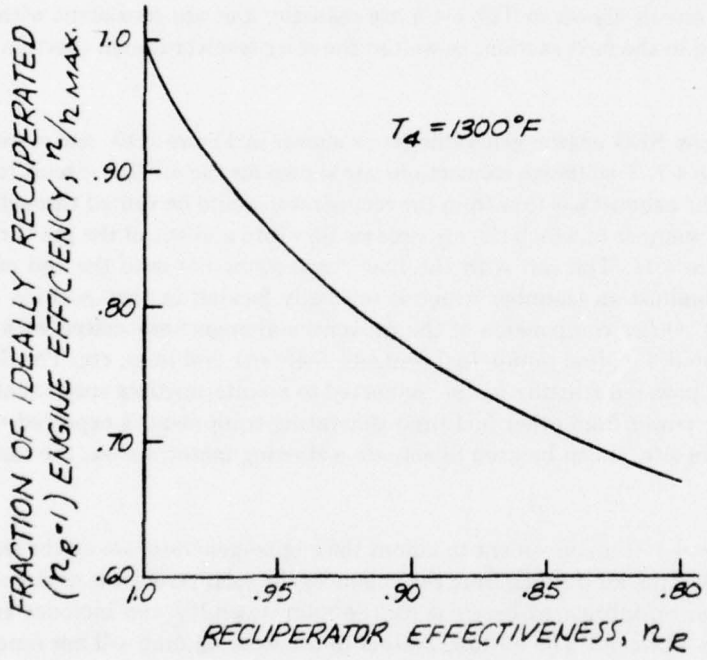

FIGURE 4.9 EFFECT OF RECUPERATOR EFFECTIVENESS ON ENGINE EFFICIENCY

engine-generator system efficiency as a fraction of the efficiency achievable with ideal recuperation ($\eta_R = 1$), versus the recuperator effectiveness for a turbine inlet temperature of 1300°F and optimum turbine inlet pressure. The figure shows that increasing the recuperator effectiveness from 0.85 to 0.95, for example, would increase the overall engine-generator efficiency by a factor of about 1.2 and reduce the collector area by the same factor. We expect that the increased recuperator size and cost associated with this effectiveness increase would be more than offset by the reduced collector size.

The values for gear box and alternator efficiency in Table 4.5 are those achieved by the SDIH unit. The efficiency value for miscellaneous losses is intended to account for power to the oil-pump, the instruments and controls, and the solar collector drive. Finally, the pressure drop allowances for the air flow circuit shown in Table 4.5 are realistic, and are consistent with the recuperator design described in the next section, as well as the solar receiver design (Section 4.3) and ducting sizes.

The configuration of the SEG engine-generator set is shown in Figure 4.10, and a weight breakdown is given in Table 4.7. Two flange connections are shown for the air flow circuit to the solar receiver and return. The exhaust gas flow from the recuperator would be vented through the exhaust line indicated. The manner in which the air streams flow into and out of the gas turbine assembly is shown in Figure 4.11. The can with the flow connections fits onto the end of the assembly in place of the combustion chamber which is normally located in that position on a conventional fuel-fired unit. Other components of the conventional engine associated with fuel firing would also be eliminated, i.e., fuel pump, fuel controls, fuel tank and lines, etc. The SDIH unit is started by a battery-powered starting motor connected to an intermediate speed shaft on the gear box. Since electric power from other fuel-fired generating equipment is expected to be available at the SEG system site, it can be used to actuate a starting motor; hence, the battery would not be required.

As described in Section 4.1, it is convenient to mount the engine-generator set on the rear of the parabolic reflector, so that the air ducting from the engine to the solar receiver is as simple as possible. The SDIH unit has oil-lubricated bearings for the rotor assembly and includes an oil pump for forced feed of the lubricant. The oil-lube system in the existing unit will not function properly over the large changes in orientation that will be associated with movement of the parabolic reflector. Therefore, the detailed design of this oil-lube system would have to be reviewed and modified to permit the unit to operate in the various orientations that would be expected. An alternative to such modifications would be to mount the engine-generator set on the fixed portion of the collector structure and make connections to the parabolic dish via flexible lines. This would be difficult, however, since the connecting lines are relatively large, hot and insulated.

4.2.4 Recuperator Design

The size of the recuperator unit shown in Figure 4.10 was established by preliminary design calculations based on use of the plain plate-fin heat transfer surface shown in Figure 4.12 (Figure 10-30 in Reference 5). Other salient features of the recuperator design are summarized in Table 4.8.

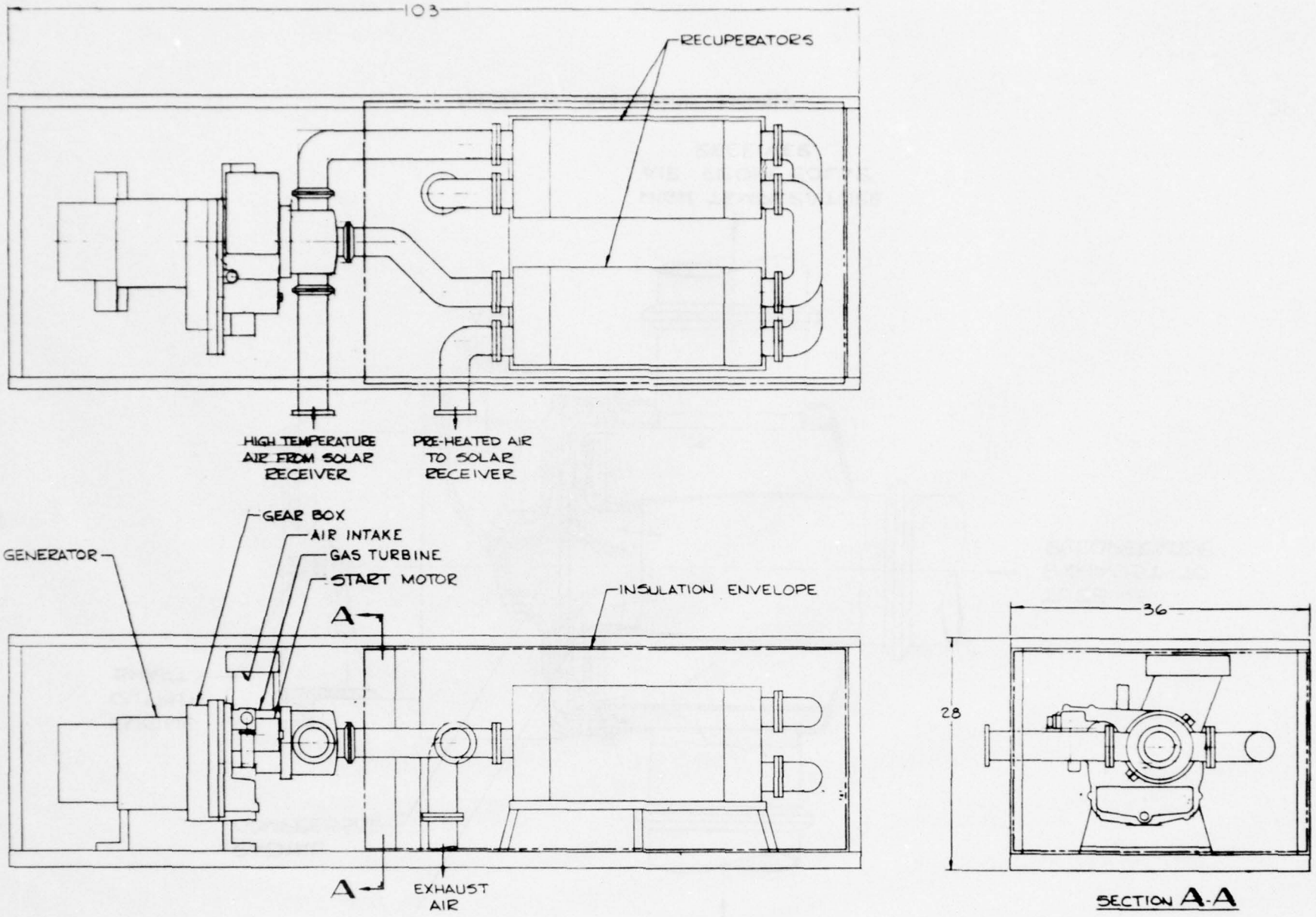

FIGURE 4.10 SEG ENGINE - GENERATOR SET

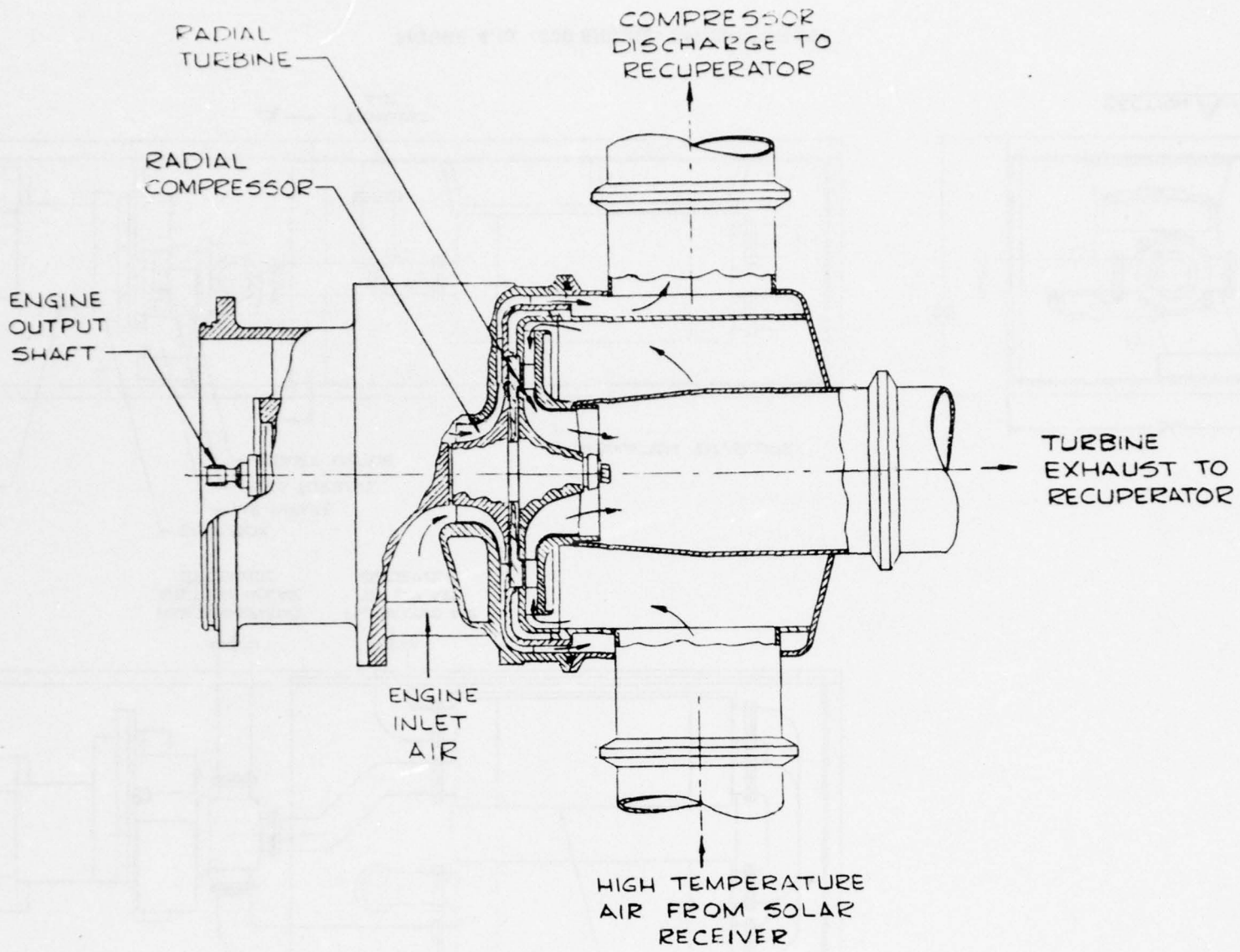

FIGURE 4.11 GAS TURBINE ASSEMBLY

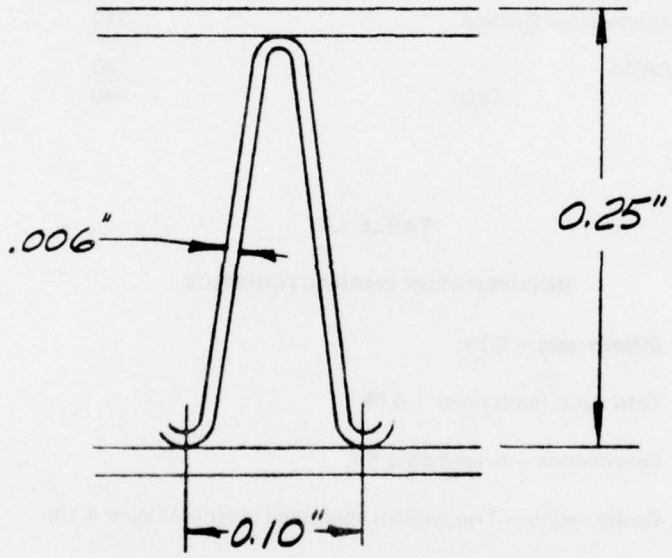

FIGURE 4.12 RECUPERATOR HEAT TRANSFER SURFACE

TABLE 4.7

GT ENGINE-GENERATOR SET WEIGHT ESTIMATES

	Weight (lb)
Gas Turbine, Reduction Gear and Engine-Mounted Accessories	90
Generator	170
Frame	100
Controls, Electrical Components	40
Other Accessories	80
Recuperator and Ducting	340
Insulation	60
Total	880

TABLE 4.8

RECUPERATOR CHARACTERISTICS

Effectiveness – 0.95

Total $\Delta p/p$ (both sides) – 0.05

Construction – Brazed plate-fin

Configuration – Two sections connected in series (Figure 4.10)

Approximate dimensions – 12" x 14" x 30" (each section)

Fin Thickness – 0.006"

Weight (stainless steel construction) – 280 lb

A recuperator with an effectiveness of 0.95 and with pressure drop requirements and operating temperature levels similar to those of the unit depicted in Figure 4.7 was designed and built by AiResearch Division of Garrett Corporation. It was tested successfully at the NASA Lewis Research Center in connection with a program on closed Brayton-cycle systems for generation of electric power in spacecraft.(6) The cycle used a helium-xenon gas mixture and operated over a power output range of 2-15 kWe. High effectiveness plate-fin heat exchangers (0.95 and higher) are also used in some industrial processes. Clearly, the feasibility of achieving thermal/pressure-drop performance like that projected for the recuperator of the SEG system has

been demonstrated. However, the open-cycle SEG engine utilizing air as the working fluid poses corrosion-related problems that were not a factor in the AiResearch exchanger test program. Achieving satisfactory mechanical integrity of the SEG system recuperator might require some developmental effort. The temperatures at which the recuperator would operate (i.e., 270°-1000°F) are sufficiently high that oxidation rates of metals of construction can be significant. Construction of the recuperator from a material such as 347 stainless steel (which was used in the AiResearch unit) may be satisfactory if section thicknesses are made sufficient to allow for oxidation erosion effects. If not, more costly high-temperature alloys would have to be employed.

4.2.5 Engine Off-Design Performance Characteristics

The engine operating parameters of Table 4.5 refer to a nominal design-point condition and correspond to a solar flux of 275 Btu/hr-ft². As noted in Section 3, lower solar flux will produce a lower turbine-inlet temperature and reduced power output, in accordance with Figures 3.6 through 3.9. Figure 4.13, which shows the estimated engine-generator part-load characteristics, is based on the engine component characteristics. To develop the figure, the following simplifying assumptions were made:

(1) The engine inlet temperature and pressure are constant,
(2) The compressor discharge pressure is constant,
(3) The turbine flow characteristic is like that of a choked nozzle,
(4) The compressor and turbine efficiencies are constant, and
(5) The recuperator effectiveness is constant.

The first assumption is appropriate for the preliminary estimates of interest at this time. The effects of ambient pressure and temperature variations are not large for climatic conditions that might be expected at Naval bases in any case. Their effects on engine performance are generally well known or can be determined by more detailed analysis. The assumption of constant compressor-discharge pressure is consistent with the characteristics of the radial compressor over the range of flow rates that occur in part-load operation. The third and fourth assumptions are approximations that, when used to estimate part-load performance of fuel-fired engines, led to results that compared well with their performance data. Thus, Figure 4.13 shows a comparison of part-load efficiency data for the SDIH Gemini engine (described in Section 4.2.2) with projections based on assumptions 1 through 4. The part-load efficiency of the AiResearch GTP 30-141 engine (a nominal 100-hp output engine of similar design) is also shown. The figure demonstrates general agreement between the actual and projected results.

Finally, the assumption of constant recuperator effectiveness is reasonable because the changes in air flow rate through the engine at part load are not large (see Figure 3.6, for example).

4.3 Receiver Design

The primary incentive to utilize a modest concentration level to achieve the required operating temperature range is that less precision is required in the tracking system and the surface contours of the parabolic dish concentrator. An additional benefit is that the heat fluxes in the receiver cavity are relatively modest, thereby simplifying the heat exchanger surfaces required to transfer the absorbed solar energy to the air flow with a low temperature drop. This is in contrast to those systems using very high levels of solar concentration (2000:1), where the heat fluxes can be very high and the design of the receiver a major technical problem.

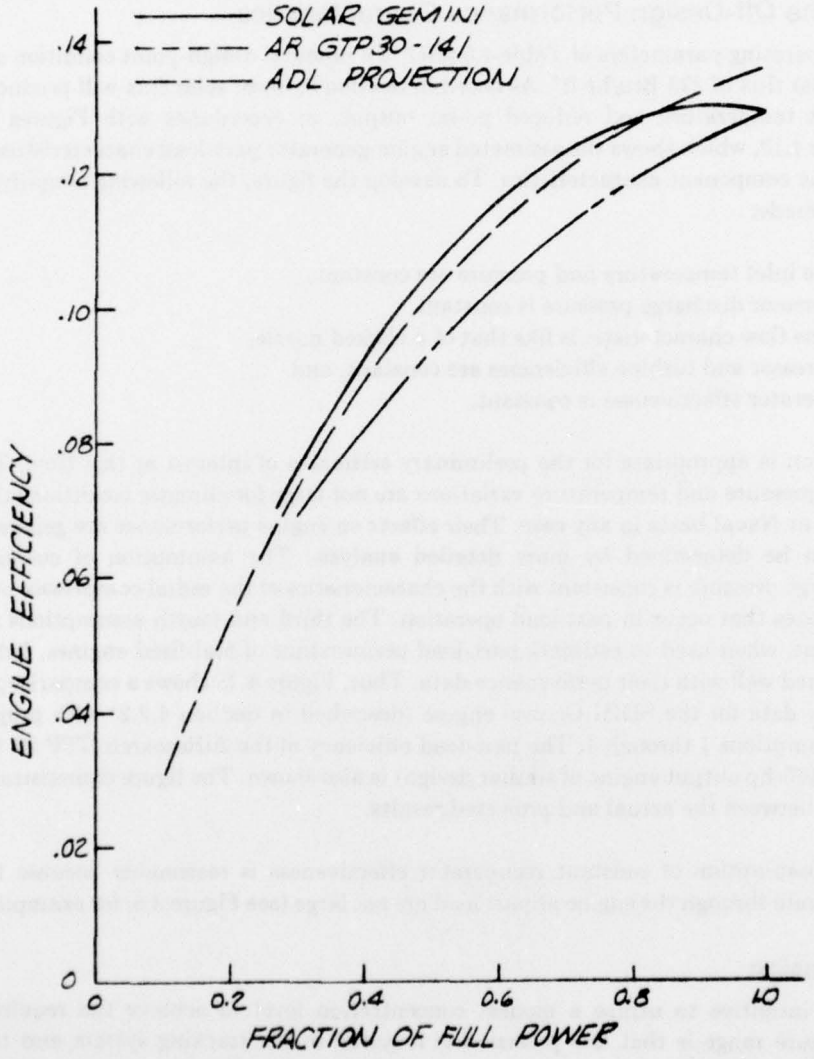

FIGURE 4.13 PART-LOAD EFFICIENCY OF SMALL GAS TURBINES

4.3.1 Design Goals

Under design conditions, the total heat flux to the receiver aperture is 152,000 Btu/hr, of which about 80% is transferred to the air stream and 20% lost by reradiation, conduction through the insulation, and convection.

The design goals for the receiver design were:

- A physical configuration using heat-transfer surfaces which are similar to those used commercially for other applications; this would, in turn, result in a design which can be built at low cost in relatively small quantities;
- An air-side pressure drop amounting to less than 4% of the design peak pressure level or a Δp of about 1.2 psid;
- Absorbing surface to air stream temperature drops of 70°F or less. This is to limit cavity temperature levels and, hence, reradiation losses;
- Compact size to reduce shading of the reflector; and
- Low weight to minimize structural requirements.

4.3.2 Design Configuration

A number of design options that showed promise of satisfying the above requirements were considered.

The preferred receiver design is shown in Figure 4.14. This option appeared to make best use of commercial heat exchanger design and resulted in a relatively light-weight structure to withstand the 40-psi pressure levels in the air stream. It consists of 56 round tubes (1 inch O.D.) placed around the circumference of the receiver cavity. Air from the recuperator flows into the inlet manifold which distributes the air to the tubes. After flowing through the tubes, the heated air enters an outlet manifold and then to a central return duct which connects to the engine. The ducts connecting the engine to the receiver pass up the center of the receiver cavity. This is done to minimize the length of ducting required and any shading effects the ducts would have on the concentrator surface.

To achieve the goals of a low receiver surface to air stream temperature differential, the tubes will require internal finning with an area enhancement of about 5 to 1. Candidate arrangements for such internal finning are shown in Figure 4.14. With these arrangements (particularly option b), area enhancements well in excess of those required could be achieved.

Most common steels are not appropriate for use at the operating temperatures required of the receiver. However, the maximum operating temperature (1350°F) is well within the range of specialty steels such as those used in gas tubes. Table 4.9 lists some of the candidate materials for tube fabrication. The preliminary designs assumed the use of Type 347 stainless steel, which is commonly used in moderately high-temperature applications. If the internal finning arrangement of Figure 4.14b is used, the fins would be made of nickel due to its relatively high thermal conductivity (k = 48 Btu/hr-ft-°F versus about 10 for Type 347 stainless).

The major heat loss from the receiver is by reradiation through the receiver aperture. The conduction losses off the sides and top of the receiver can be greatly reduced by use of an effective

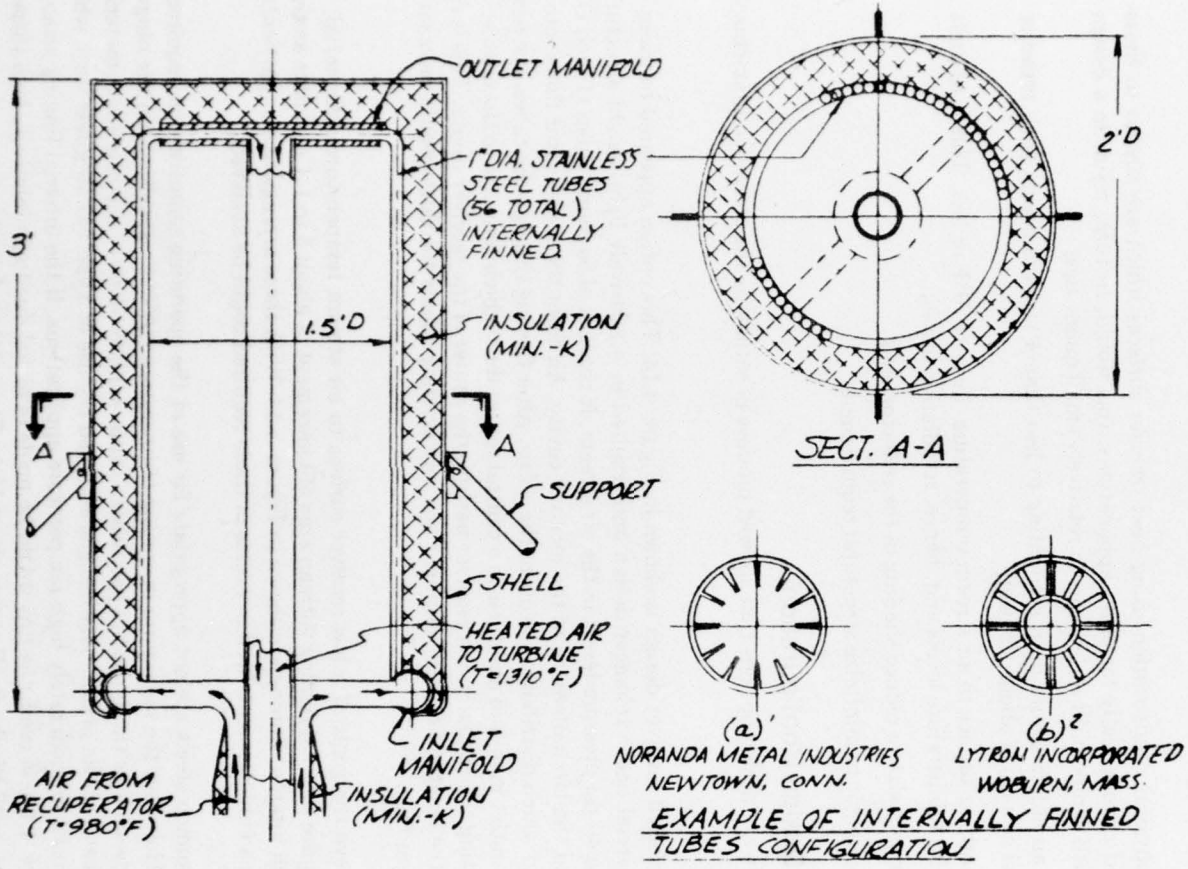

FIGURE 4.14 RECEIVER CAVITY DESIGN

TABLE 4.9

CONSIDERATIONS FOR SELECTING CANDIDATE RECEIVER TUBING MATERIALS

Alloy	Temperature at Which 3.4 kpsi Produces Rupture in 1000 hr (°F)	Hot Corrosion Resistance	Tube Fabricability	Brazing Compatibility	Cost (50,000 ft Lots) $/100 ft
Type 347 stainless steel	1550	Poor	Good	Good	34
Type 430 stainless steel	1200	Poor	Good	Good	
Armco 21-6-9	1450	Poor	Good	Good	
L-605	1800	Good	Good	Good	111
N-155	1750	Good	Good	Good	87
AiResist 213	1775	Excellent	Fair	Good	
Inconel 600	1600	Fair	Good	Good	37
Incoloy 800	1500	Fair	Good	Good	37
Incoloy 825	1600	Fair	Good	Good	41
Hastelloy X	1800	Good	Good	Good	107
Hastelloy C	1700	Fair	Good	Good	
Hastelloy F	1700	Good	Good	Good	
Inconel 625	1800	Good	Good	Good	46
Inconel 718	1600	Good	Fair	Good	
Udimet 500	1850	Fair	Poor	Good	
Udimet 700	1850	Fair	Poor	Good	
TD Nickel	2000	Poor	Good	Fair	

thermal insulation. Figure 4.15 shows the thermal conductivity of several types of thermal insulation suitable for use at the temperature levels associated with the receiver. MIN-K 1301 has a significantly lower thermal conductivity than the more commonly used fibrous ceramic-type insulation forms. To keep the overall diameter of the receiver to a minimum (and, thereby, minimize shadowing effects), MIN-K 1301 was selected as the insulation for the preliminary design.

4.3.3 Design Parameters

The resultant preliminary design parameters for the receiver are:

Aperture Area — 1.76 ft^2

Aperture Diameter — 1.5 ft

Overall Diameter — 2 ft

Heat Collected — 124,150 Btu/hr

Number of Tubes — 56

Area Enhancement — 5 to 1

Tube and Manifold Material — Type 347 Stainless

Size — 1 inch O.D., 0.028 inch wall

Insulation Type — MIN-K 1301

Insulation Thickness — 2 in.

Air Temperature In — 980°F

Air Temperature Out — 1310°F

Air Flow Rate — 355 cfm

Pressure Drop — < 0.5 psi

Average Tube to Air Temperature Drop — 55°F

4.3.4 Temperature Distribution

As indicated on Figure 4.14, the air entering the receiver is at a temperature of 980°F and the air leaving the receiver is at the design temperature of 1310°F. The average temperature of the air stream in the receiver is, therefore, about 1150°F. If the heat flux on the walls were uniform, the corresponding average wall temperatures would range from 1035 to 1365°F with an average of about 1200°F. In actuality, the heat flux at the lower (and colder) end of the receiver will behigher than at the hot end, which would reduce the peak wall temperature below that indicated above, probably to about 1340°F.

In any case, the average wall temperature in the receiver is about 100°F below the peak cycle temperature. Therefore, the efficiency curves of Section 3.3, which were based on the receiver operating at a constant temperature equal to the peak engine temperature (i.e., 1300°F), will tend to be somewhat conservative (i.e., the reradiation heat losses will be lower than estimated).

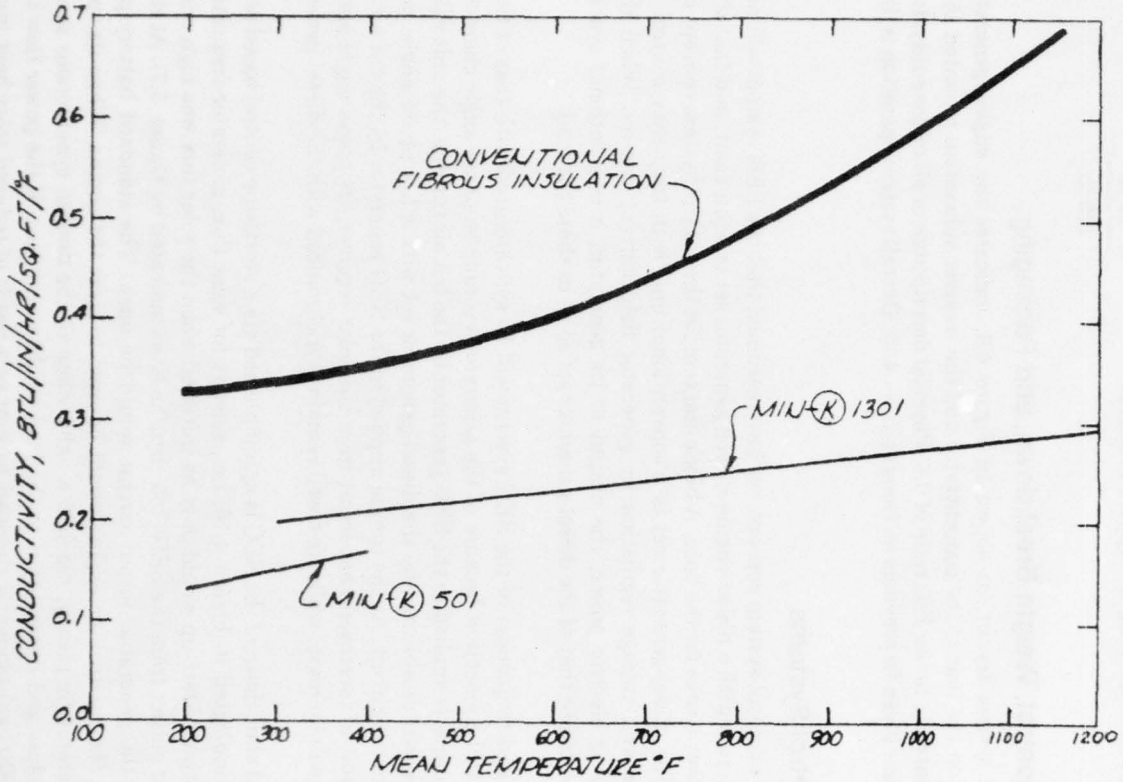

FIGURE 4.15 CONDUCTIVITY OF THERMAL INSULATIONS

4.3.5. Weight Breakdown

The weight of the receiver assembly is estimated to be 175 pounds as broken down below:

Internally Finned Tubing	82 lb
Manifolds	10 lb
Insulation	68 lb
Outer Sheathing & Support Brackets	15 lb
	175 lb

4.4 System Control, Weight Breakdown, and Packaging

The overall system layout, as shown in Figure 4.6, indicates the engine/generator subsystem mounted on the rear of the concentrator and the receiver subsystem mounted 15 feet in front of the concentrator for an F/D ratio of 0.6. Physical descriptions of all major subsystems and their operation were given in previous sections (4.1 — 4.3). Overall system operation is discussed below.

4.4.1 Control Systems

In evolving a control system concept, we have assumed that the SEG system will normally operate in conjunction with a diesel-engine-driven generator set or equivalent, and that the latter is the primary power source for the base. A block diagram for the control system concept is shown in Figure 4.16. The diesel-generator set is a conventional unit with frequency control via fuel input modulation and voltage regulation by generator field current control. When the SEG system is producing electric power, the output of its generator, a conventional synchronous machine, is connected to that of the diesel-generator set so as to share the load.

The speed (and frequency) of the SEG system will be synchronized with that of the diesel set via this electrical connection because of the generator's torque vs phase angle characteristic. Thus, when low torque is applied to the SEG generator by the hot air turbine, the unit will run at the synchronous speed established by the diesel-generator set with a low phase-angle, and with low power input to the circuit. As the torque applied to the SEG generator by the hot air turbine increases as a result of increased heat input from the solar receiver, its phase angle and power input to the load will increase, while its speed remains synchronized with the diesel-generator.

Start-up and shut-down of the SEG is accomplished via a start/stop control based on inputs from the sensors indicated in Figure 4.16, i.e., sensors for solar flux, generator frequency, and electric power output. Start-up would only be initiated when the solar flux was high enough to produce net power output from the SEG (180 Btu/hr-ft^2 as indicated by Figure 3.7). At start-up, the contactor in the generator output circuit would be open. The standard battery-powered starting motor in the gas turbine engine would be used to start the engine. When its speed, as indicated by generator frequency, reached a value close to the desired synchronous speed, the contactor would close and power input to the load would commence. If the power flow into the circuit from the SEG subsequently dropped to zero as a result of reduced solar heat input, the contactor would open to prevent power absorption by the SEG. The engine would be shut down by bypassing the air flow around the solar receiver, i.e., by stopping the heat input.

Short-term start-stop cycling can be avoided by use of a time delay in the start/stop control.

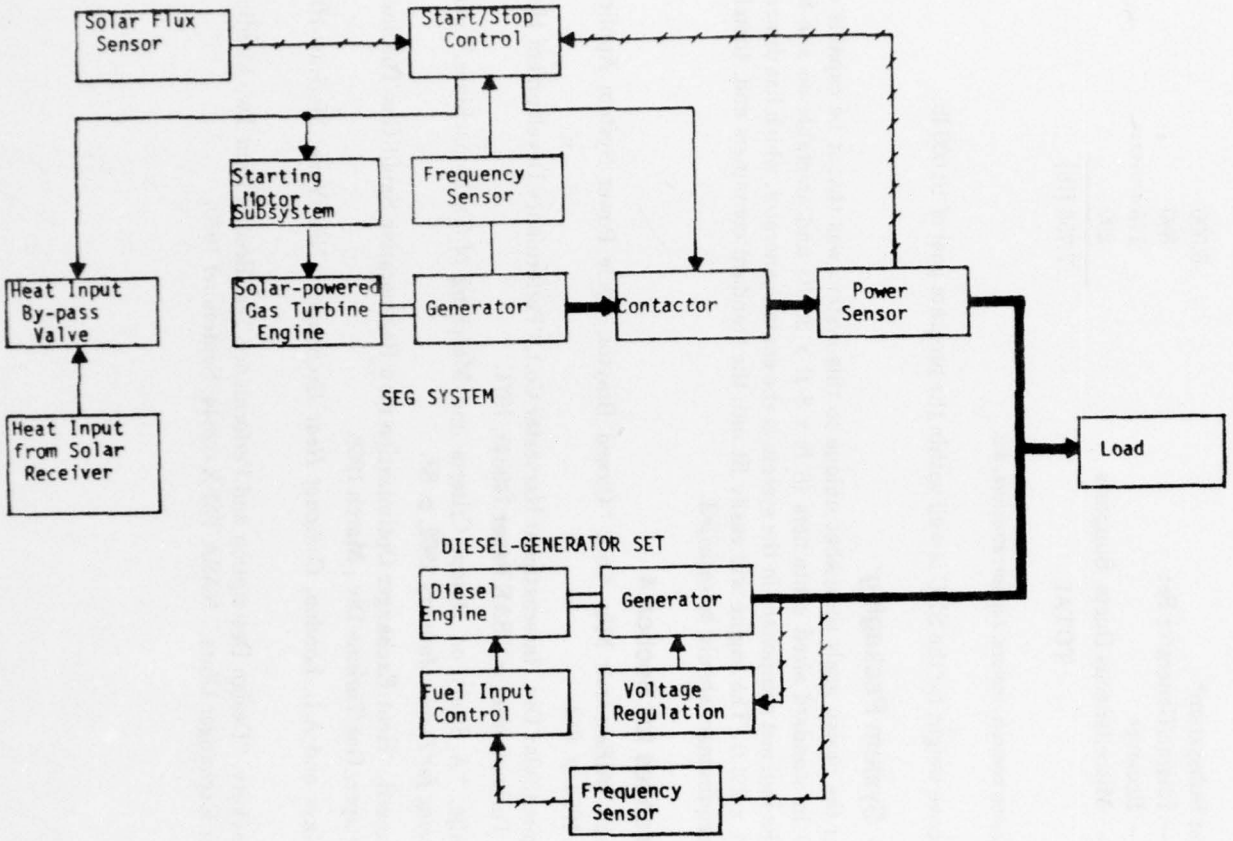

FIGURE 4.16 BLOCK DIAGRAM, INTEGRATED DIESEL-ELECTRIC/SEG CONTROL SYSTEM CONCEPT

4.4.2 Weight Breakdown

The weight breakdown for each of the subsystems was given in the previous sections. These weights are summarized below for the total system.

Concentrator Subsystem*	6,500
— Engine/Generator Set	880
— Receiver	175
— Miscellaneous Ducts, Supports	200
TOTAL	7,755 [lb]

*Including tracking controls, motors, support structure, etc.

The above weight for the SEC is well within the program goal of 10,000 lb.

4.4.3 System Packaging

One of the design goals somewhat unique to this system was that it be capable of being transported in standard sized containers (8 ft x 8 ft x 20 ft) and erectable on site by Navy Seabees. The bulkiest component in the system is the engine/generator, which has dimensions of 8.5 ft x 3 ft x 2.3 ft. The engine will easily fit into the standard containers and, therefore, the packaging requirement should be satisfied.

4.5 References for Section 4

1. A. Pietsch (AiResearch Mfg. Co.), "Closed Brayton Cycle Power System Applications," IECEC, 1969, p. 642.
2. C. Rodgers (Solar Div., International Harvester Co.), "Performance Development History — 10 kW Turboalternator," SAE Paper 740849, 1974.
3. O.E. Balje, "A Study on Design Criteria and Matching of Turbomachines," *Journal of Engineering for Power*, January 1962, p. 83.
4. E.P. Demetri, "Heat-Exchanger Optimization for a Regenerative Small-Gas-Turbine Cycle," ASME paper, Gas Turbine Div., March 1968.
5. W.M. Kays and A.L. London, *Compact Heat Exchangers*, New York: McGraw-Hill, 1958, p. 197.
6. G.N. Kaykaty, "Design Description and Performance Test Results from Two Identical Brayton Heat Exchanger Units," NASA TM X-52844, September 1970.

5. COST ESTIMATES

None of the major subsystems within the solar-fired Brayton-cycle engine are presently in commercial production. This complicates the task of estimating the cost of the system. In making our cost estimates we made the following assumptions:

- The production rate of power units is 1000 per year;
- All subsystems are developed and ready for manufacture; and
- All SEG systems are being produced exclusively for the remote and advanced-base Navy applications.

In reality most of the subsystems would require a significant R&D effort to bring them to a stage where they could be produced with a high degree of confidence. This is particularly true for the regenerative Brayton-cycle engine. Contacts with one potential manufacturer of this engine indicate development effort of about $1-2 million.

In developing cost estimates for the system, contacts were made with potential subsystem manufacturers and component suppliers. Information from potential equipment suppliers was combined with Arthur D. Little estimates to result in the overall subsystem cost estimates discussed below.

5.1 Concentrator System

Contacts with manufacturers of microwave antennas indicate that the cost of the concentrator subsystem in very limited quantities would be roughly $75,000. This cost includes all the reflector, controls, motors, etc. associated with the concentrator arrangement of Figure 4.1. Antennas with overall size and contour parameters similar to the concentrator of baseline design are, in fact, now being made. It is not clear that the basic fabrication technique now used to construct antennas (discussed in Section 4.1) would be greatly modified for the relatively low production quantities being considered. The projected reduction in costs to a level of $24,000 therefore results from a higher and consistent level of production, *but* still at a level which does not warrant the use of large-scale production equipment ("hard tooling," such as stamping presses).

5.2 Engine/Generator

A flame-fired 10-kWe engine/generator using an open Brayton-cycle engine will be made for the Army by SDIH at a cost of about $14,000 in quantities of 1000 per year. This engine differs from that required for the solar-fired engine in that it does not have a recuperator. On the other hand, the solar-fired engine does not need the combustion chamber, fuel system, and some of the controls of the flame-fired unit. Our engine/generator cost estimate is $12,000, which assumes that the net result will be a small decrease in engine/generator costs over that of the Army flame-fired unit.

5.3 Receiver

The primary cost factors in the receiver assembly are the purchase of the internally finned tubes and their assembly into the inlet and exhaust manifolds. Our cost estimate of $3,000 for the receiver reflects manufacturers' estimates for the major purchased materials used in the receiver and their experience in fabricating heat exchangers similar to the SEG design.

5.4 Cost Summary

A summary of the system cost estimate is indicated below.

Concentrator Subsystem	$24,000
Engine/Generator	12,000
Interface Controls	2,000
Receiver & Connecting Lines	4,000
TOTAL	$42,000

5.5 Future Cost Reductions

The modest production level of 1000 units per year does not allow for the large reductions in the cost of the subsystems which would occur if mass production techniques could be used. As a practical matter, the Navy alone could probably not represent a sufficiently large market to warrant large-scale production. It is instructive, however, to roughly estimate the cost of the power system if it were to be mass-produced.

The concentrator subsystem represents a major share of the power unit cost. The concentrator is very similar in size and function to the heliostats being proposed for the "power tower" solar thermal power concept. Cost estimates for these heliostats reflect the assumption of mass production. The resultant cost estimates for heliostats are $7-$10 per square foot (depending on design and ERDA contractor). This unit area cost would result in a concentrator cost of $5,000-$7,000, which is about one fifth of that estimated for the preliminary design.

It appears, therefore, that substantial reductions could be made in the cost of the system if all or some of the required subsystems were produced in large numbers for other applications.

6. PRELIMINARY ECONOMIC ANALYSIS

The economics of the SEG is a function of several factors, including:

Annual power produced (kWh),

Initial cost,

Maintenance requirements,

Cost and availability of power from alternative sources,

Interest rates,

Operational life, and

Non-economic issues (logistics, etc.).

The single most important performance parameter influencing the SEG's economics is the annual energy production measured in kWh. The analysis of this preliminary design stresses SEG operation under design conditions during clear days. As indicated in Figure 3.9, on a clear day in June (32° latitude), the SEG will provide about 87 kWh of electricity. The annual output will vary from location to location, depending on local climatic and insolation conditions. As indicated in Figure 3.7, the SEG output is quite sensitive to variations in direct insolation level. Therefore, calculating annual power output requires a rather detailed definition of the hourly variations in *direct* solar flux and a corresponding calculation of power output and its variation in time. Such calculations would require weather and solar insolation tapes for specific potential locations and a computer-based analysis to calculate engine performance on a continuous basis. For purposes of a *preliminary* rough estimate of annual power output, we have made the following assumptions:

- SEG output is proportional to the number of sunshine hours, as indicated in the Climatic Atlas; and
- A geographical location with solar radiation levels typical of Albuquerque, New Mexico.

The above assumptions will tend to result in an optimistic estimate of power output since:

- A very favorable location was selected, based on possible hours of sunshine (3420 hours); and
- The reduction in efficiency of the SEG with decreased direct insolation is not taken into account (i.e., output is assumed proportional to total flux, and the reduced proportion of direct radiation as insolation levels decrease is not considered).

Based on the above assumptions, the annual power output of the SEG will be approximately 25,000 kWh.

The annual charges associated with operating the SEG include:

- Interest
- Depreciation

- Insurance*
- Taxes*
- Operation and maintenance

For a system with a 20-year useful life, the capital charges will range below 10-15%, depending on interest rates. Capital charges will increase to 15-25% if the useful equipment life is only 10 years. The costs associated with routine maintenance and repair are assumed to equal 5% of the original investment due to the relatively complex nature of the concentrator/receiver and the engine/generator. Achieving this modest O&M cost goal would require designing all components to achieve very high reliability for this type of equipment. Based on the above, the cost of power can be projected by assuming

Cost of Power = (Annual Capital Cost + Annual O&M Costs)/25,000 kWh.

The cost of power calculated above is summarized in Table 6.1 for initial costs corresponding to both the low production case ($42,000 per unit) and the high production cost scenario ($12,000 per unit).

Table 6.1 indicates the cost of power from the SEG as a function of the annual capital charges for equipment with an operational life of 10-20 years. At 10% the cost of power from the SEG would be about 25.2¢/kWh. This compares with 5-20¢/kWh for power from a diesel power plant.

Table 6.1 also indicates the cost of power assuming the possible cost reduction indicated in Section 5 which might occur if critical subsystems comprising the SEG system were produced in large quantities. In this case, the cost of power would drop to 7.5¢/kWh, to 14.4¢/kWh, which compares favorably with that from small diesel power plants.

TABLE 6.1

POWER COST FROM SEG
(O&M Cost = 5% of Investment)

Annual Capital Charges* (%)	Low Production Case (Unit Cost = $42,000)		High Production Projection (Unit Cost = $12,000)	
	Annual Charges** ($)	Power Cost (¢/kWh)	Annual Charges** ($)	Power Cost (¢/kWh)
10	6,300	25.2	1,800	7.2
15	8,400	33.6	2,400	9.6
20	10,500	42.0	3,000	12.0
25	12,600	50.4	3,600	14.4

*Interest and depreciation.
**Annual charges include O&M costs.